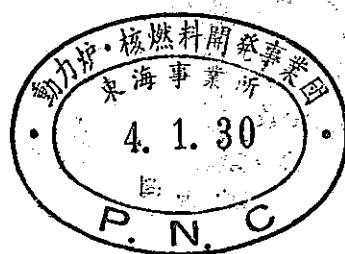


*IRRADIATION PERFORMANCE TEST OF  
PuO<sub>2</sub>-UO<sub>2</sub> FUELS BY SAXTON REACTOR*



*Power Reactor and Nuclear Fuel Development Corporation  
Japan*

#### Notice

This report is only prepared for examination in the internal materials. Enquires about copyright and reproduction should be addressed to the Head of Technical Information Service, Power Reactor and Nuclear fuel Development Corporation. Japan.

Irradiation Performance Test of  $\text{PuO}_2\text{-UO}_2$  Fuels

by Saxton Reactor

H. Akutsu

M. Koizumi

Power Reactor and Nuclear Fuel Development Corporation

Abstract

Mixed oxide ( $\text{PuO}_2\text{-UO}_2$ ) fuel rods (four rods and one assembly containing 68 rods) were irradiated to certificate irradiation performance of proto-typed fuel by Saxton Reactor to peak burnups of up to 8,050 MWD/MTM.

Linear power level was from 200 to 500 watts/cm. After irradiation, post-irradiation examinations were conducted in Battelle's Columbus Laboratories (BCL). The post irradiation examinations were consisted of visual examination, profilometry, gamma scanning, fuel and clad metallography, burnup analysis, hydride analysis in claddings and clad strength tests. These examinations showed that the overall performance of the  $\text{PuO}_2\text{-UO}_2$  fuel was satisfactory.

## I. INTRODUCTION

Power Reactor and Nuclear Fuel Development Corporation (PNC) has jointed the Saxton Core III program planned by Westinghouse. The objective of participation was to certify the irradiation performance of the PNC plutonium fuels under the condition of proto-type PWR (Saxton Reactor). PNC fabricated four fuel rods ( $4\text{wt}\%\text{PuO}_2$ ) for evaluation under high power condition and one subassembly containing 68 plutonium fuel rods ( $5\text{wt}\%\text{PuO}_2$ ) for under low power condition.

Saxton Core III reached critical on July 15, 1969.

The initial power operation of Core III started on December 11, 1969. The final power operation was at 15 MWt on May 1, 1972, when the reactor was shut down. The Saxton reactor remained shutdown from March to November 1971 for fuel examinations and etc. During this period, PNC plutonium fuels were loaded in the Reactor.

Battelle's Columbus Laboratories (BCL) provided technical assistance in evaluating the irradiation performance of these fuel rods by performing a postirradiation examination (PIE) of the rods.

PNC submitted one complete assembly and four single rods from Westinghouse assemblies to BCL for the PIE. These were shipped from the Westinghouse Saxton Reactor to the BCL Hot Laboratory Facility at West Jefferson, Ohio. PNC designated twelve rods from the assembly. These twelve rods and the four single rods were examined for the PIE.

## II. FUELS

Fuel rod design was carried out based on the design criteria of Saxton Core-II plutonium fuel rod.

The cladding is 0.993 cm outer diameter, 99.1 cm length (include end plugs) and 0.058 cm wall thickness.

The plutonium concentration is 4.0 wt% for C-1, C-2, C-3 and C-4 fuel rods which were assembled in the Westinghouse assembly, and 5.0 wt% for the rods charged in PNC assembly.

The fuel pellets were sintered to the density of  $92 \pm 1.5$  % theoretical density. The diameters of some pellets were grinded with a centerless-grinder to the appropriate diameter. Pellet-clad diametral gap size is 0.018 cm. The nominal plenum length is 5.08 cm which is enough to accomodate the fuel stack expansion and released fission gases (Xe and Kr). The spring in the plenum was used to prevent pellets to move in the cladding under transportation. The spring strength is not enough to prevent the fuel stack expansion under irradiation.

Measured values of fuel rod parameters after fabrication are listed for C-1, C-3, 25, 41 and 43 fuel rods in Table 1.

The tolerance of plutonium fissile concentration,  $\text{PuO}_2$  spot size, fuel density and diameter are less than those restricted by the hot channel factors of Saxton Reactor. The restriction to the impurities of pellet was required to make sure the reliable fuel pin performance. The specification to the pellet disfigurement is same to that used for Saxton plutonium fuel of Westinghouse.

### III. REACTOR OPERATING HISTORY AND IRRADIATION CONDITION

#### Reactor operating history

PNC four fuel rods and one assembly were irradiated by the Saxton Core III irradiation history illustrated in Figure 1.

The irradiation was started on November 19, 1971 and shut down on May 1, 1972.

#### Irradiation condition

The location of PNC plutonium fuel rods in the Saxton Core III are shown in Figure 2. The C-2 rod is in the assembly 503-10-8. The location of C-1, C-2, C-3, C-4, 25, 41 and 43 rods in the assemblies are illustrated in Figures 3, 4 and 5. The power histories of each fuel rod are essentially the same, however the power level is slightly different from each other. The power histories were shown in Figure 6 at the planes of the metallographies in the postirradiation examination and listed in Table 2.

#### IV. POST IRRADIATION EXAMINATION

##### Removal of rods from assemblies

The upper nozzles were removed from Westinghouse assemblies 503-17-9 and 503-17-2. Fuel rods C-1, C-2, C-3 and C-4 were then removed and transferred to the Hot Cell for postirradiation examination (PIE). Since the upper nozzle to the PNC assembly, 503-10-8, was welded in place, the nozzle was cut away using an abrasive cutting disc. Fuel rods 14, 25, 26, 32, 37, 39, 40, 41, 43, 46, 65 and 66 were then removed and transferred to the Hot Cell for PIE.

#### 1. NON-DESTRUCTIVE EXAMINATION

##### 1-a Visual examination

The overall appearance of the unshrouded fuel assembly was shown by photographs (Photo. 1) of the as-received assembly. A comprehensive documentation of the surface features of fuel rods 25, 41 and 43 was made using a Bausch and Lomb Stereomacro-scope. Photographs of selected areas show the distribution and nature of clad deposits and the appearance of corrosion fibers, of welds and weld heat-affected zones at the end closures and of other unusual features such as clad ridging.

As a typical example, photographs of the rod 41 is shown in Photo. 2.

##### 1-b Dimension measurement

##### The length of fuel rods

The pre and post-irradiation fuel rod lengths are listed

in Table 3 with the calculated  $\Delta L(L-L_0)$  and  $\Delta L/L_0$ . All fuel rods measured were lengthened by irradiation.  $\Delta L$  is from 0.42 to 0.94 mm and  $\Delta L/L_0(\%)$  is in the range from 0.042 to 0.095. These values are considerably small.

#### Profilometry

Profilometer measurements were made on six fuel rods.

From the data of profilometry,  $\Delta D/D_0$  were calculated and shown in Figure 7 through 9 as the function of axial length of a fuel rod. The diameters of all fuel rods are decreased. The diameter changes increase gradually from the ends to the center of fuel rods. The cladding were yielded somewhat with the aid of strong external (coolant) pressure ( 140 atms).

#### 1-c Gamma scanning

The gross gamma activity was measured along the length of fuel rods C-1, C-2, C-3, C-4, 14, 25, 26, 32, 37, 39, 40, 41, 43, 46, 65 and 66. The data of gross gamma activity are shown in Figure 10 for rods C-1 and 41. In the case of C-1 rod, activity profile shows two irregular portions, which just corresponds the locations of the grids.



## 2. DESTRUCTIVE EXAMINATION

### 2-a Fission-gas analysis

Fuel rods C-1, C-3, 25, 41 and 43 were punched and the free gases within the rods collected and analyzed.

The analyzed gas constituents are shown in Table 4.

The isotopic composition of the Krypton and xenon percent in the gas is presented in Table 5.

### 2-b Fuel and clad sectioning

Sectioning diagrams for fuel rods C-1, C-3, 25 41 and 43 appear in Figure 11. Rods were sectioned as indicated on these diagrams.

### 2-c Fuel and cladding metallography

Generally all rods were not irradiated at high temperature except the rod C-1, therefore fuel restructuring change is not remarkable. The conditions of the examined fuel rods are summarized in Table 6. Concerning the fuel rod (C-1) central void and columnar grain growth are observed which diametral fractions are reasonable values by evaluation from our fuel performance calculation code. Fuel-clad interaction and ridging behavior were not observed. Longitudinal section photography (C-1) showed interesting behavior of gap geometry between both pellets at high temperature zone by mal-loading of single side dished pellets.

### Fuel pellet densification

Fuel void fraction measurements were conducted using a image analysis device. The samples are:

C-1	Transverse section	C-1(T)
C-3	Transverse section	C-3(T)
43	Transverse section	43(T)
43	Longitudinal section	43(L)

The results of measurement are illustrated in Figures 12 through 15 with the estimated fuel temperature distributions. The data points are comparatibly dispersed, because void fraction measurement technique with a image analysis is still under development.

However, the void fractions after irradiation are almost under the level of initial void fractions, that means some degree of fuel densification occurred. The fuel void fractions and densities of pre and post-irradiation are listed in Table 7 with the rod powers and burnup data. The fuel void fractions and densities in the table are the average values on the sectioning areas.

Fuel density increase is the biggest in C-3(T) section (3.5%), and the smallest in 43(L) section (1.06%).

Consequently, the effects of rod power, fuel temperature and burnup on the fuel densification are not evident.

Cladding metallography showed no particular phenomena. With respect to hydration of cladding the hydrides were not almost observed in this test comparing in other irradiation tests.

## 2-d Alpha autoradiography

The objective of this operation was to determine the distribution of alpha-emitting species (plutonium) in the irradiated fuel samples. Samples consisted of prepared metallographic specimens. A listing of the alpha autoradiographs taken and their features is given in Table 8.

The beta-gamma autoradiographs are also included in this tabulation. The photographs of  $\alpha$  and  $\beta$ - $\gamma$  autoradiography are shown in photo. 4, 6, 8, 10 and 14.

## 2-e Fuel burnup

### Analysis by heavy element isotopic and Neodymium-148 determinations

Results of isotopic-abundance and cesium-137 analysis are shown in Table 9. Sample locations, weights (1.27 cm sections), and burnup calculations are outlined in Table 10.

Burnup calculations were based on the formula

$$F_T = \frac{F' \cdot 100}{U' + P' + F'}$$

where  $F_T$  = total heavy element atom percent burnup

$F'$  = fissions/atom U-238

$U'$  = atoms U/atom U-238

$P'$  = atoms Pu/atom U-238

The number of fissions was determined from the number of Nd-148 atoms divided by the fraction of Nd-148, 0.0169, resulting from Pu-239 fission.

Transuranic analysis for Np-237, Pu-236 and Am-241, 243 are listed in Table 11.

Radial drilling; Burnup analysis

The fuel was drilled concentrically and in succession with drills of 4.14, 5.63, 6.79 and 7.67 mm diameter. A fifth outer sample consisted of the remaining outer annulus of fuel adjacent to the clad. Each sample was dissolved and analyzed as described in the previous burnup analysis section. Results were calculated and are included in Table 10 and plotted in Figure 16.

Burn-up radial distribution measured with the rod 41 is comparatively proportional to the neutron flux distribution in the rod. The burn-up in the periphery of the pellet is higher than that in central region.

2-f Cladding hydrogen analysis

Transverse sample rings were cut from rods 25 and 43 for hydrogen analysis of the cladding by high temperature vacuum extraction. The hydrogen content was measured in two opposing quarter segments of the sample rings by vacuum extraction at 1000°C.

Results are shown in Table 12. The precision was determined to be 4 percent at the 32 ppm hydrogen level from analysis of National Bureau of Standards titanium standards.

2-g Tube burst test

Tube burst tests were made on samples of Zircaloy cladding from fuel rods 25 and 43. Tests were conducted on one specimen from each of the two rods and failure-strain measurements were made at maximum rupture points on each specimen.

The temperature for these tests was controlled to  $385 \pm 3^{\circ}\text{C}$  at the center of the gage length during testing.

The nominal rate of pressurization during the test is  $140.62 \text{ kg/cm}^2/\text{min}$ . The pressure-volume curve generated in the test is then corrected for system expansion and a specimen pressure-expansion ( $\Delta$ -volume) curve constructed.

The rod identification number, the specimen location as measured from the bottom of the rod and specimen test-temperature data are tabulated in Table 13 with the data of post-irradiation.

The constructed pressure - $\Delta$ volume curve for rods 25 and 43 are given in Figure 17.

The  $\Delta$ -volume equivalent to the 0.2 percent yield stress is calculated using the formula

$$V = 1.57 D_o^2 \cdot L_o \epsilon_p$$

where  $\Delta V$  = specimen volume change

$D_o$  = specimen nominal inside diameter

$L_o$  = specimen length

$\epsilon_p$  = diametral strain = 0.002

The 0.2 percent offset yield stress is then calculated using the formula.

$$\tau_1 = P_1 \cdot D_o / 2t$$

where  $\tau_1$  = 0.2% offset yield (hoop) stress

$P_1$  = pressure obtained from the pressure -  
 $\Delta$ volume curve at which 0.2% offset yield  
occurs

$t$  = specimen nominal wall thickness

The failure stress is calculated using the similar formula,

$$\tau_2 = P_2 \cdot D_o / 2t$$

The 0.2 percent offset-yield and failure stresses are also tabulated in Table 13. The failure strain is defined as the increase in circumference divided by the original circumference. The results are shown in Table. The 0.2% yielded stress and failure stress are both increased after irradiation. The failure strain is remarkably reduced by approximately a half. The brittleness of Zircaloy clad is considered to be increased.

#### 2-h Tube tensile test

The tube tensile test was conducted on a 152.4 mm long specimen in an Instron tensile-test machine. Each end of the specimen was held in a grip so that a 101.6 mm length was free to deform. The test temperature was  $385 \pm 3^\circ\text{C}$ . The cross head speed was 1.016 mm per minute, yielding a nominal strain rate along 101.6 mm section of 0.01 per minute. The data obtained are given in Table 14. The results of tensile tests indicated the same tendency as that of the burst tests.

2-j Ring tensile test

The ring tensile test was also conducted using an Instron tensile test machine and a grip assembly which permitted a radial load to be applied to a tube cross section. The test temperature was  $385 \pm 3^{\circ}\text{C}$  and the cross head speed was 0.508 mm per minute.

The uniform elongation is defined as the strain at maximum load. The total elongation is defined as the strain at which a sharp load drop occurs.

The outside diameter before testing is used as the gage length in elongation calculations. The ultimate tensile strength is defined as the maximum load divides by the original cross sectional area.

The yield stress is defined as the load at 0.2 percent strain offset also divided by the original cross sectional area. The maximum reduction in width is defined as the maximum change in width (axial rod direction) divided by the initial width. The maximum increase in outside diameter (O.D.) is defined as the difference between the greatest post test O.D. and the initial O.D., divided by the initial O.D.

The data obtained are listed in Table 14.

## VI. CONCLUSION

PNC irradiated plutonium fuels (four rods and one assembly) in the Saxton Reactor Core III. All fuel rods were irradiated safely. The four rods (C-1, C-2, C-3 and C-4) contained in the Westinghouse assemblies were irradiated at the position close to the reactor center, and reached to the maximum burnup of 8,050 MWD/T. The rod powers of this rods were in through from 300 to 500 w/cm.

PNC assembly (68 rods) were irradiated by comparatively low power of 370 watts/cm. The average burnup achieved is about 4,000 MWD/T. The post-irradiation examinations conducted in BCL indicated that the claddings did not lose their integrity and little hydrides were detected.

The diameter measurement of fuel rods indicated interesting results, that is, the diameters of each rod decreased by 0.2 to 0.7 percent in length. Maximum decrease occurs just in the middle of each fuel rod.

Fuel restructuring is maximum in the case of C-1 fuel rod. The other fuel rods showed almost no fuel restructuring except some degree of grain growth in the center region.

The clad strength tests, burst test and tensile test showed the irradiation hardening of zircaloy cladding. The 0.2% offset yield strength and failure stress were increased by the factor of ~5. Failure strain was decreased by a half compared with the pre-irradiation data.



Reference

- 1) W. R. Smalley, "Evaluation of Saxton Core III Fuel Materials Performance," WCAP-3385-57, July 1974.
- 2) C. C. Busby and K. B. Marsh, "High Temperature Deformation and Burst Characteristics of Recrystallized Zircaloy-4 Tubing," WAPD-TM-900, January 1970.
- 3) "Irradiation Effects on Structural Alloys for Nuclear Reactor Applications," ASTM STP484.
- 4) V. Fidleris, "Uniaxial In-Reactor Creep of Zirconium Alloys," J. of Nucl. Mater. 26 (1968) 51-76.

Table 1 Fuel Rod Parameters

Fuel Rod No.	C-1	C-3	25	41	43
Plutonium concentration(w/o)	3.98	3.98	4.85	4.85	4.85
Pellet Diameter (mm)	8.577	8.577	8.579	8.579	8.579
Pellet Highth (mm)	9.510	9.510	9.601	9.601	9.601
Dish Diameter (mm)	7.52	7.52	7.433	7.433	7.433
Dish Depth (mm)	0.348	0.348	0.355	0.355	0.355
Fuel Density (%T.D)	91.54	91.54	91.80	91.80	91.80
PuO <sub>2</sub> /PuO <sub>2</sub> ·UO <sub>2</sub> (w/o)	3.98	3.98	4.85	4.85	4.85
O/M	2.008	2.008	1.997	1.997	1.997
Adsorbed Gas (μℓ/g)	20	20	20	20	20
Clad Material	Zry-4	Zry-4	Zry-4	Zry-4	Zry-4
Clad Inner Diameter (mm)	8.729	8.729	8.734	8.734	8.734
Clad Outer Diameter (mm)	9.938	9.938	9.924	9.924	9.924
Fuel Stack Length (mm)	911.5	910.0	906.5	911.0	908.0
Fuel Rod Total Length (mm)	991.80	991.86	991.88	991.76	991.78
Plenum Length (mm)	48.10	49.70	54.45	49.40	53.15
Clad Maker	WH-07	WH-09	W.H-60	M.W-07	M.W-01
He Pressure (atom)	1	1	1	1	1

Table 2 Irradiation Conditions

Fuel Rod No.	25	41	43	C-1	C-3
Reactor Power (MWt)	23.5	23.5	23.5	23.5	23.5
Rod Power(w/cm) Priod 5	360	200	370	500	300
Priod 6	370	200	370	490	320
Burnup (MWD/MTU)	—	3430	5570	8050	5890
Irradiation Time (day)	92.9	92.9	92.9	92.9	92.9
Assembly	503-10-8	503-10-8	503-10-8	503-17-9	503-17-9

Table 3 Comparison of Rod Length between Pre and Post Irradiation

Rod No.	Pre-Irradiation	Post-Irradiation								
	PNC	BCL			GE-VNC*			GE-VNC**		
	Total Length Lo(mm)	Total Length L (mm)	$\Delta L$ (mm) (=L-Lo)	$\Delta L/Lo$ (%)	Total Length L (mm)	$\Delta L$ (mm) (=L-Lo)	$\Delta L/Lo$ (%)	Total Length L (mm)	$\Delta L$ (mm) (=L-Lo)	L/Lo (%)
25	991.88	992.38	0.50	0.050	992.25	0.55	0.055	992.8	1.10	0.111
37	991.70	992.31	0.61	0.062						
40	991.80	—	—	—						
41	991.76	992.63	0.87	0.088						
43	991.78	992.72	0.94	0.095						
C1	991.80	992.35	0.55	0.055	992.20	0.42	0.042	992.8	1.02	0.103
C2	991.78	992.27	0.49	0.049						
C3	991.86	990.40	0.54	0.054						
C4	991.80	992.25	0.45	0.045						
								993.8	2.00	0.202

\* Measured at Vallecitos Nuclear Center of GE

\*\* Based on Neutron Radiography

Table 4 Plenum-Gas Analysis (Volume percent)

Rod	H <sub>2</sub>	He	CH <sub>4</sub>	H <sub>2</sub> O	O <sub>2</sub>	N <sub>2</sub>	Ar	CO <sub>2</sub>	Kr	Xe	Xe/Kr
C-1	0.17	42.1	0.01	0.1	0.10	0.63	0.03	0.01	3.50	53.5	15.3
C-3	0.02	97.8	0.01	0.1	0.02	0.07	0.02	0.01	0.14	1.88	13.4
25	0.01	96.4	0.01	0.4	0.04	0.29	0.01	0.01	0.20	2.70	13.5
41	0.01	95.3	0.01	0.4	0.42	2.68	0.03	0.01	0.08	1.04	13.0
43	0.01	96.0	0.01	0.4	0.03	0.52	0.05	0.01	0.19	2.78	14.6

Table 5 Krypton and Xenon Isotopic Analysis (Volume percent)

Rod	Krypton				Xenon			
	83	84	85	86	131	132	134	136
C-1	17.6	29.5	7.0	45.9	13.1	19.8	26.1	41.0
C-3	18.5	29.4	7.5	44.6	12.9	22.7	26.1	38.3
25	18.5	29.3	6.9	45.3	12.7	20.6	27.5	39.2
41	18.5	29.6	6.9	45.0	13.1	20.6	29.3	37.0
43	18.2	29.3	6.8	45.7	12.6	19.7	27.9	39.8

Table 6 Fuel Restructuring and Temperature

Fuel Rod No.	41( <sup>*</sup> T)	43(T)	C-1(T)	C-3(T)
Rod Power (w/cm)	190	360		310
<sup>*</sup> Restructuring (mm)				
Equiaxed Region	—	—	2.740(64%)	—
Columnar Region	—	—	2.244(52%)	—
Central Void Region	—	—	0.234(5.5%)	—
Temperature (°C)				
Clad Surface	300	320	340	310
Clad Inner	320	360	390	350
Fuel Surface	440	590	650	550
Fuel Center	900	1820	2310	1560
Burnup (MWD/MTU)	3430	5570	8050	5890

\* Distance from Fuel Center

\*\* Transverse Section

Table 7 Fuel Density of Pre and Post-Irradiation

Rod No.	Pre-Irradiation		Post-Irradiation		Rod Power (w/cm)	Burnup (MWD/MTU)
	Void Fraction (%)	Density (% T.D)	Void Fraction (%)	Density (% T.D)		
43(T)*	8.20	91.80	5.49	94.51	(1) 354.3 (2) 357.6	5570
43(L)	8.20	91.80	7.14	92.86	(1) 287.0 (2) 285.0	4480
C-1(T)	8.46	91.54	6.28	93.72	(1) 449.5 (2) 465.9	8050
C-3(T)	8.46	91.54	4.96	95.04	(1) 305.1 (2) 288.7	5890

\* T; Transverse Section (1); Priod 5  
 L; Longitudinal Section (2); Priod 6

\*\* (1) The value During Period 5  
 (2) The value During Period 6

Table 8 Summary of Alpha and Beta-Gamma Autoradiography

Metallographic Specimen	Alpha	Beta/Gamma
C-1 (Transverse)	Dark spots indicate plutonium-rich particles in outer portions of fuel. Alpha activity in center regions is more homogeneous	Beta/gamma activity is fairly uniform in outer regions of fuel. A ring of low activity surrounds the center void in the region of columnar grain growth.
C-1 (Longitudinal)	Dark spots indicate plutonium-rich particles in outer portions of fuel. Alpha activity in center regions is more homogeneous.	There appears to be more activity in the outer region of fuel than in the fuel center.
43	Dark spots indicate plutonium-rich particles throughout fuel. There is essentially no difference in the plutonium distribution between fuel surface and fuel center.	There appears to be slightly more activity on one side of the sample. There is no difference between edge and center, however.
C3	Dark spots indicate plutonium-rich particles throughout fuel.	There appears to be a slight gradient in activity across the fuel radius, possibly because of flux depression.
41	Dark spots indicate plutonium-rich particles throughout fuel. The particles appear to be fairly large compared to those noted in other fuel samples.	There appears to be a slight gradient in activity across the fuel radius, possibly because of flux depression.

Table 9 Mass Spectrometric and Cs-137 Analysis

Sample No.	Atom Percent Abundances										Date of Pu Analysis	Atom Ratios		Cesium-137	Fission
	U-234	U-235	U-236	U-238	Pu-238	Pu-239	Pu-240	Pu-241	Pu-242	Pu-239/U-238		Nd-148/U-238	dpm/g U <sup>(1)</sup>	/g U <sup>(2)</sup>	
C-1	0.0050	0.6153	0.0186	99.3611	0.091	77.445	18.898	3.220	0.346	9/7/73	$2.77 \times 10^{-2}$	$1.49 \times 10^{-4}$	$5.93 \times 10^{10}$	$2.17 \times 10^{18}$	
C-3	0.0054	0.6443	0.0127	99.3376	0.071	81.754	15.538	2.400	0.229	9/10/73	$3.06 \times 10^{-2}$	$1.09 \times 10^{-4}$	$4.70 \times 10^{10}$	$16.22 \times 10^{18}$	
41	0.0051	0.6858	0.0074	99.3017	0.055	86.785	11.148	1.879	0.133	9/10/73	$4.29 \times 10^{-2}$	$0.64 \times 10^{-4}$	$2.54 \times 10^{10}$	$9.53 \times 10^{18}$	
43	0.0044	0.6686	0.0094	99.3176	0.064	84.008	13.489	2.256	0.183	9/11/73	$4.03 \times 10^{-2}$	$1.04 \times 10^{-4}$	$4.23 \times 10^{10}$	$15.38 \times 10^{18}$	
41-1	0.0052	0.6904	0.0073	99.2971	0.052	87.444	10.770	1.612	0.122	9/17/73	$4.30 \times 10^{-2}$	$0.53 \times 10^{-4}$	$2.51 \times 10^{10}$	$7.85 \times 10^{18}$	
41-2	0.0052	0.6880	0.0073	99.2995	0.061	87.105	10.997	1.706	0.131	9/17/73	$4.31 \times 10^{-2}$	$0.57 \times 10^{-4}$	$2.37 \times 10^{10}$	$8.47 \times 10^{18}$	
41-3	0.0054	0.6853	0.0082	99.3011	0.068	86.693	11.268	1.831	0.140	9/17/73	$4.31 \times 10^{-2}$	$0.61 \times 10^{-4}$	$2.50 \times 10^{10}$	$9.04 \times 10^{18}$	
41-4	0.0052	0.6790	0.0072	99.3081	0.057	86.745	11.417	2.039	0.142	9/18/73	$4.22 \times 10^{-2}$	$0.62 \times 10^{-4}$	$2.79 \times 10^{10}$	$9.19 \times 10^{18}$	
41-5	0.0052	0.6834	0.0084	99.3030	0.058	86.029	11.436	2.328	0.149	9/20/73	$4.31 \times 10^{-2}$	$0.78 \times 10^{-4}$	$3.04 \times 10^{10}$	$11.63 \times 10^{18}$	

(1) Measured on 8/10/73.

(2) Based on a fission yield of 1.69 percent for neodymium-148 formed from fission of plutonium-239.



Table 10 Burnup Calculations

Rod No.	Location, mm From Bottom	Sample Weight, g	Fissions <sup>(1)</sup> / Atom U-238, F'	Atoms U/ Atom U-238 U'	Atoms Pu/ Atom U-238 P'	Heavy Element Atom percent Burnup, F <sub>T</sub>	Burnup <sup>(2)</sup> in MWD/MTU
C-1	447.68 - 460.38	7.3672	0.008817	1.0064	0.03577	0.839	8050
C-3	457.2 - 469.9	7.2338	0.006450	1.0067	0.03742	0.614	5890
41	444.5 - 457.2	7.5467	0.003787	1.0070	0.04943	0.357	3430
43	447.68 - 460.38	7.5778	0.006154	1.0069	0.04797	0.580	5570
41-1	482.6 - 508.0 (Inner)	2.4851	0.003136	1.0071	0.04917	0.296	2840
41-2	482.6 - 580.0	2.0401	0.003373	1.0071	0.04948	0.318	3060
41-3	ditto	2.0286	0.003609	1.0070	0.04972	0.340	3270
41-4	ditto	1.7004	0.003669	1.0070	0.04887	0.346	3320
41-5	ditto (Outer)	1.8182	0.004615	1.0070	0.05010	0.435	4170

(1) Based on a fission yield of 1.69 percent for Nd-148 from Pu-239 fission.

(2) Assuming  $G_{wd}/mtU = F_T$  (9.6 0.3)

Table 11 Radiochemical Analysis for Transuranics  
Atom Ratios to Pu-239

Rod No.	$\mu\text{g Np-237}/$ $\text{g U}$	Pu-236	Am-241 <sup>(1)</sup>	Am-243
C-1	22.6	$1.15 \pm 1.05 \times 10^{-9}$	$5.77 \times 10^{-3}$	$2.14 \pm 1.4 \times 10^{-4}$
C-3	12.4	$1.2 \pm 1.7 \times 10^{-9}$	$4.75 \times 10^{-3}$	$< 1.4 \times 10^{-4}$
41	11.1	$3.6 \pm 5.3 \times 10^{-10}$	$3.72 \times 10^{-3}$	$< 1 \times 10^{-4}$
43	16.4	$1.3 \pm 1.0 \times 10^{-9}$	$4.49 \times 10^{-3}$	$< 1.2 \times 10^{-4}$

(1) Analyzed between 8/14/73 and 8/16/73.

Table 12 Cladding Hydrogen Analysis Data

Rod Identification	Sample No.	Location from Rod Bottom (cm)	Sample Weight (g)	H <sub>2</sub> Content cc-atm	ppm H <sub>2</sub>
25	25-A	38.10 ~ 39.37	0.3010	0.101	30
	25-B	38.10 ~ 39.37	0.2420	0.078	29
43	43-A	41.28 ~ 42.23	0.2420	0.088	33
	43-B	41.28 ~ 42.23	0.2075	0.080	34

Table 13 Tube Burst Data

Rod Identification		Location of <sup>(1)</sup> Specimen (cm)	Average Tube O.D. (mm)	Temperature (°C)	0.2% Offset Yield Stress (kg/mm <sup>2</sup> )	Failure Stress (kg/mm <sup>2</sup> )	Failure Strain (%)
25	Pre-Irrad.	—	9.924	385	18.50	27.43	61
	Post-Irrad.	40.64 to 60.96	9.550	385	50.18	54.00	10
43	Pre-Irrad.	—	9.924	385	18.50	27.43	61
	Post-Irrad.	47.31 to 67.63	9.528	385	50.05	55.29	7

(1) : As measured from the bottom of the rod.

Table 14 Tensile Data

Test	Rod No.	Temp. (°C)	Specimen Location	0.2 % Offset Yield Stress (kg/cm <sup>2</sup> )	UTS (kg/cm <sup>2</sup> )	Uniform Elongation (%)	Total Elongation (%)
Tube Tensile*	43	385	—	3400.0	5000.0	8.7(300°C)	16.0
		385	15.6 30.8cm from bottom of rod	3585.8	5239.1	3.2	7.0
Ring Tensile*	43	300	—	3594.7	5768.3	7.6	43.0
		385	40.6cm from bottom of rod	5471.2	5942.3	5.9	20.1

\* Note : These data are presented by Mitsubishi Metal Corporation (MMC).

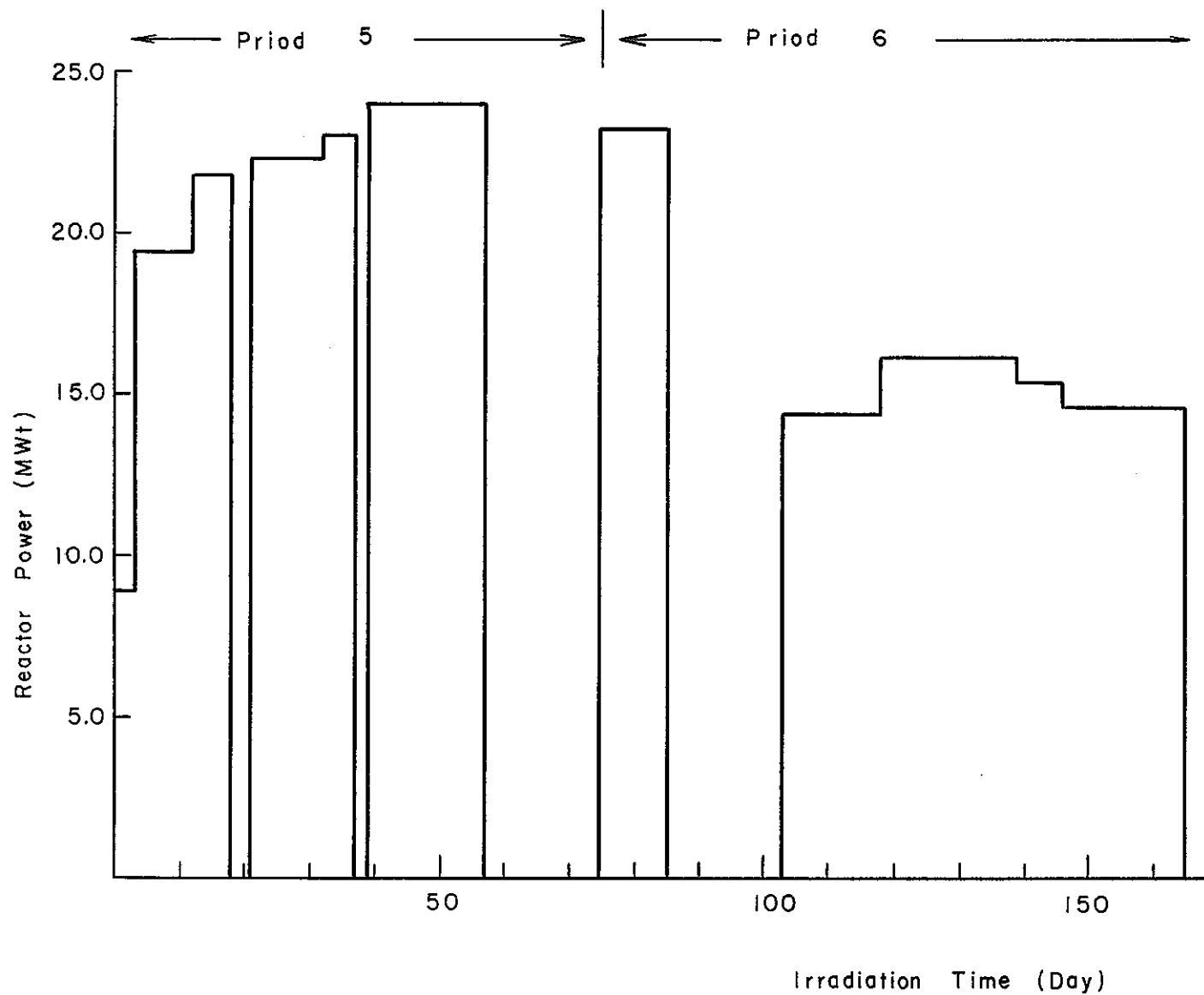


Figure 1. Reactor Operating History

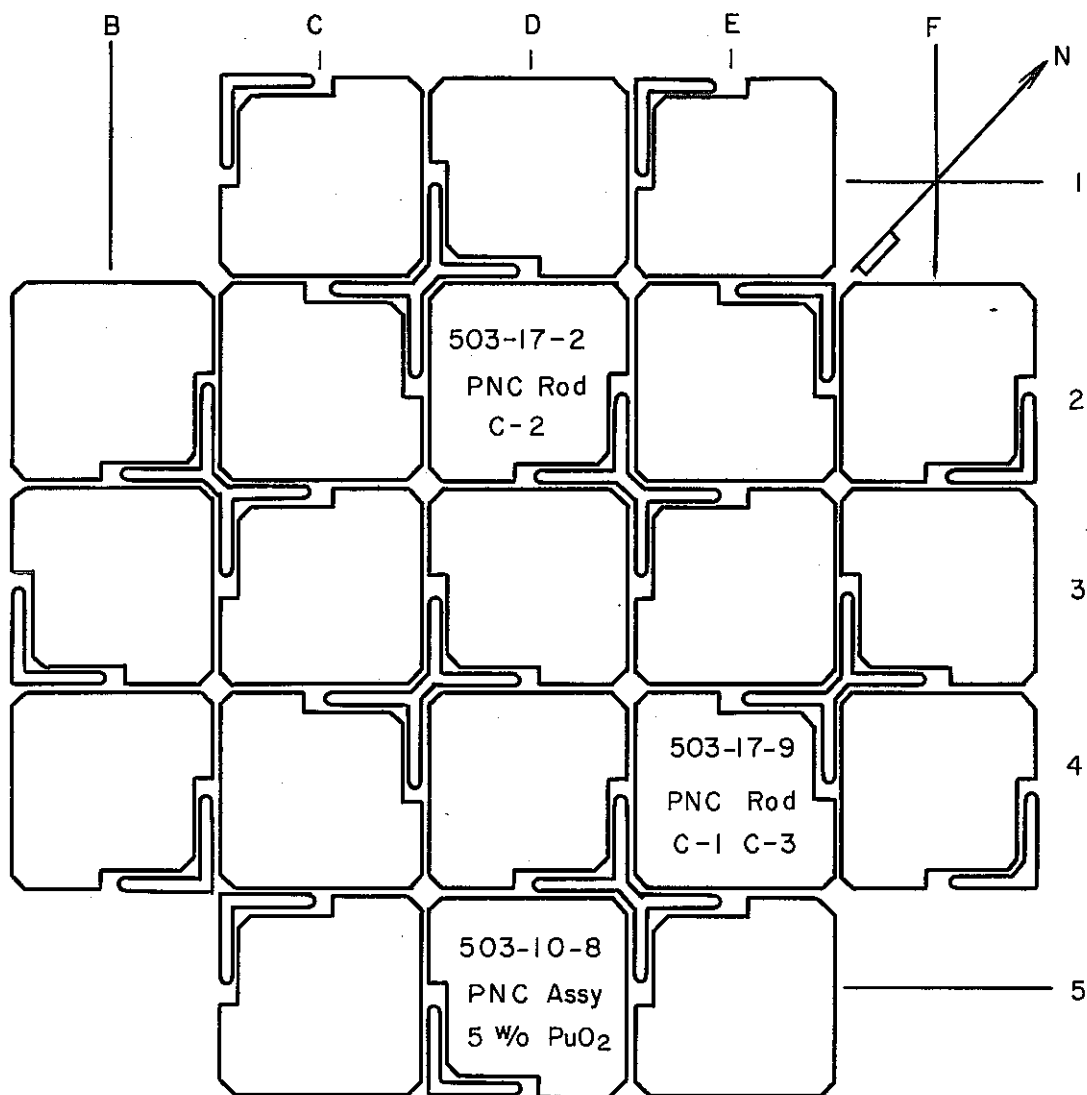


Figure 2. Fuel Configuration for Saxton Core III

Core Center

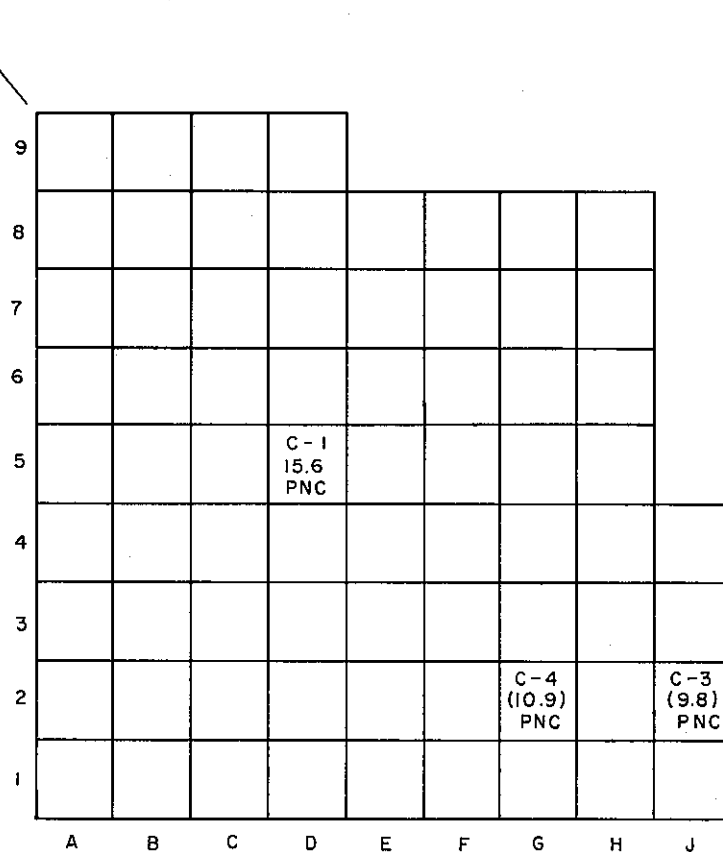


Figure 3. Assembly 503-17-9

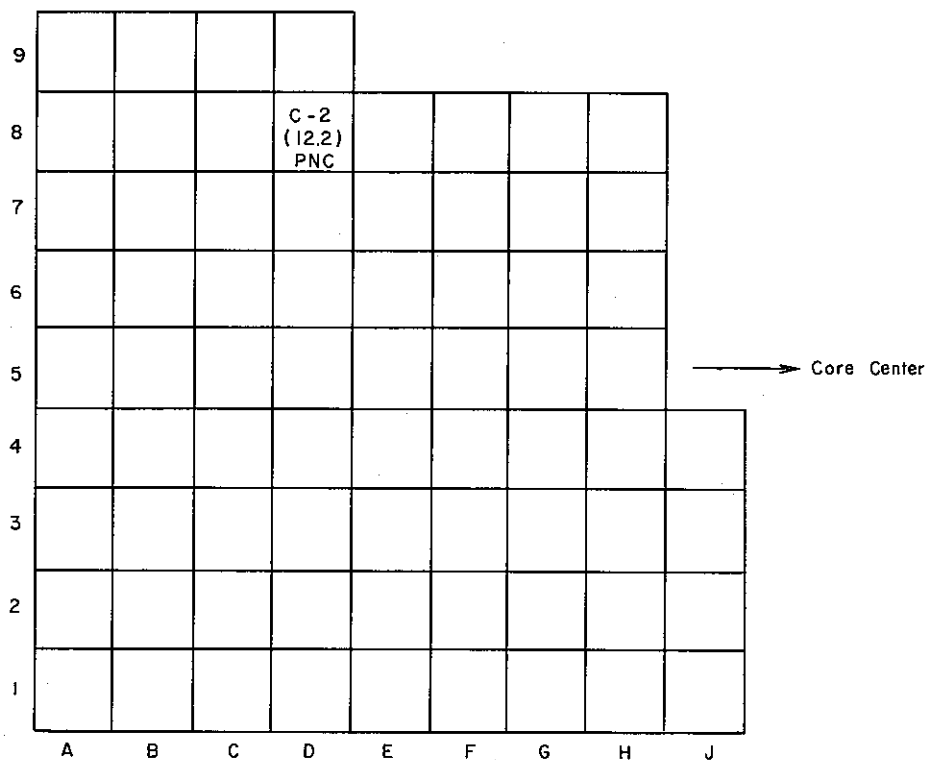


Figure 4. Assembly 503-17-2

9	Zr - 4 Bar	54	39	44	"L" Assembly 503-3-4				
8	47	56	48	30	24	17	10	6	
7	63	57	49	31	26	18	32	3	
6	64	58	50	33	27	19	11	5	
5	(FT)	46	51	34	37	20	12	42	
4	65	59	52	35	28	21	13	7	4
3	67	60	41	36	29	22	14	8	1
2	68	61	53	38	40	23	15	9	2
1	66	62	55	45	Sb - 2A (R)	43	16	25	Zr - 4 Bar
	A	B	C	D	E	F	G	H	J

Figure 5. Assembly 503-10-8

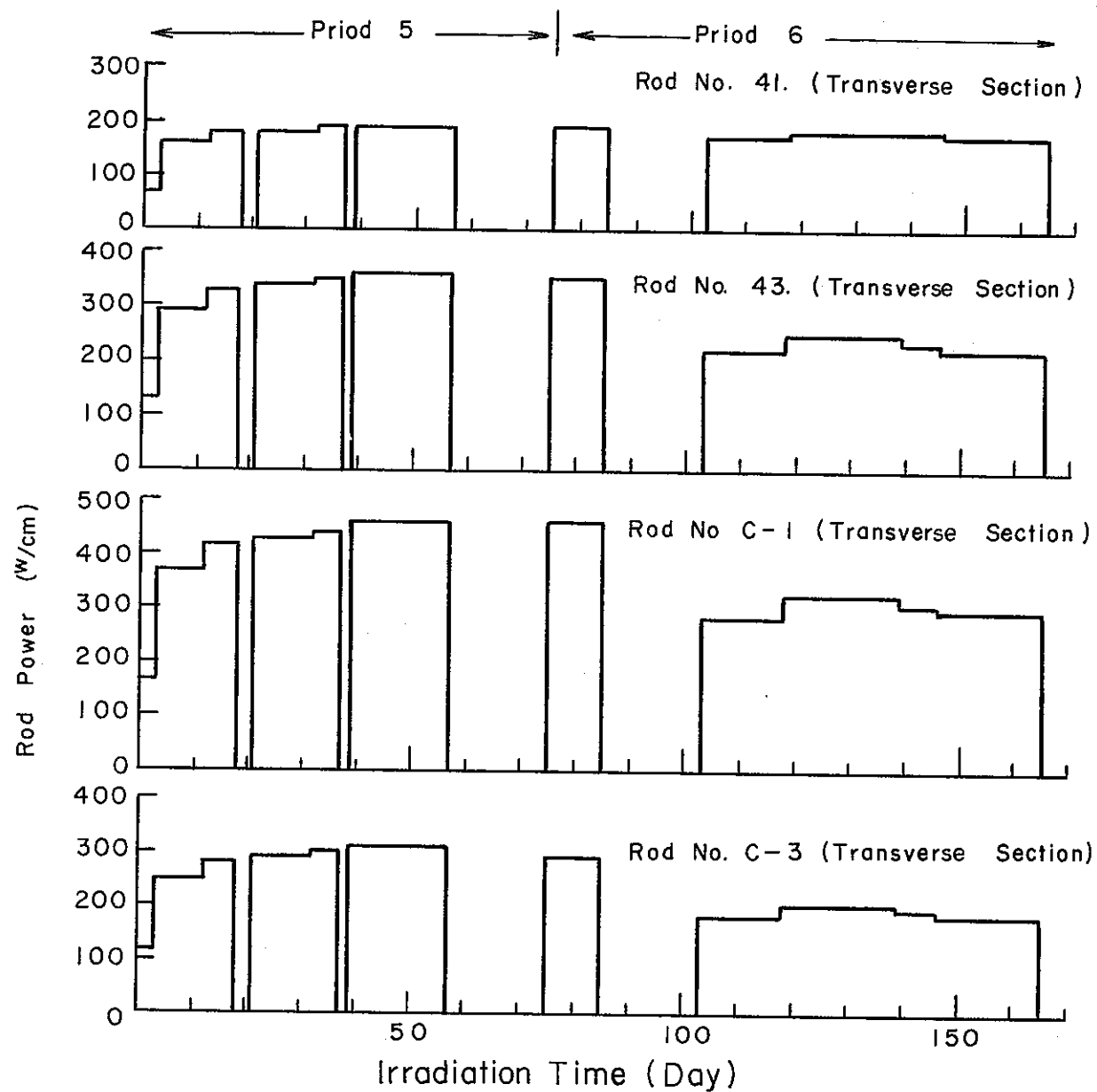


Figure 6. Power History of Rod No.41,43,C1 and C3



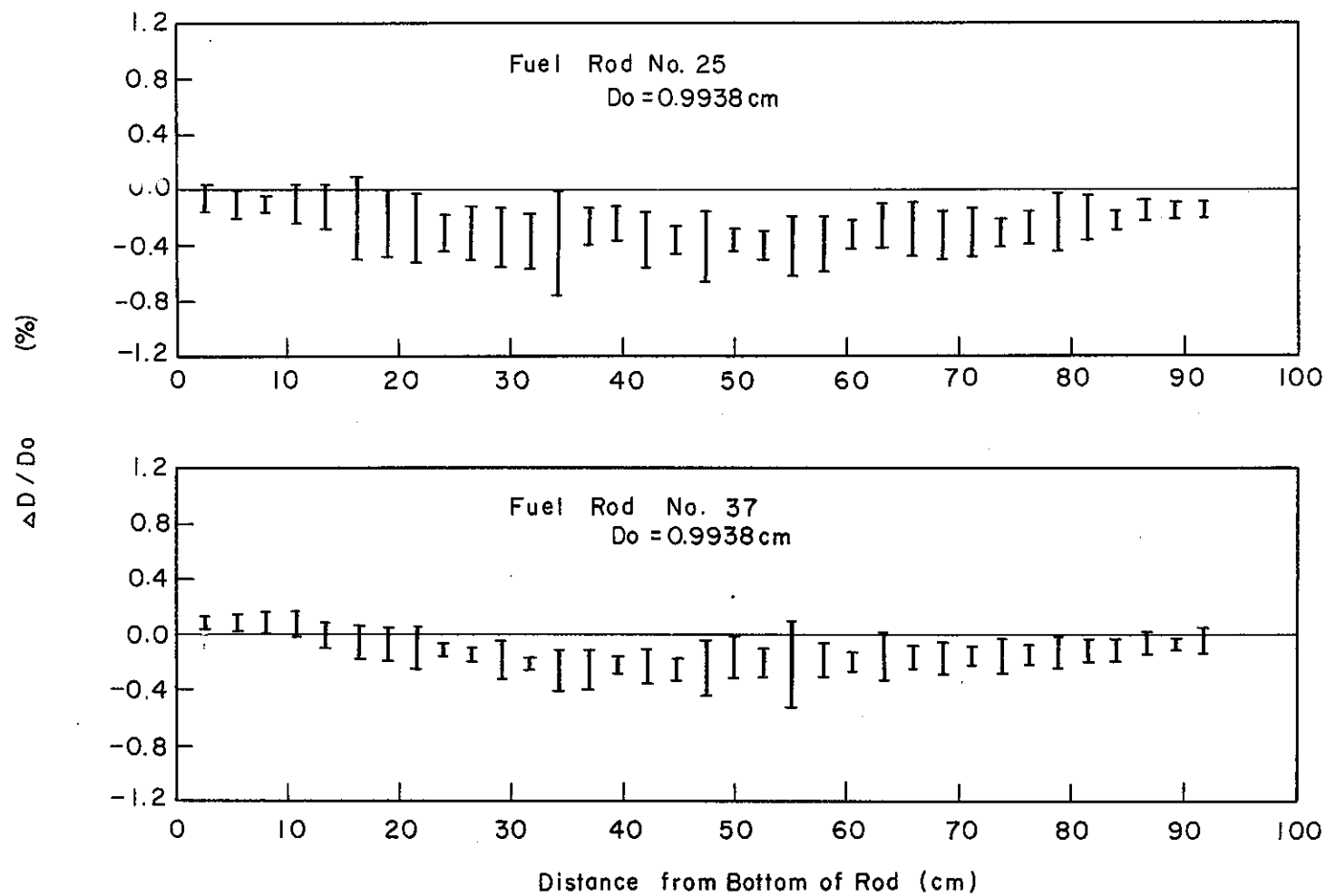


Figure 7. The Diameter Change of Rod No.25 and 37

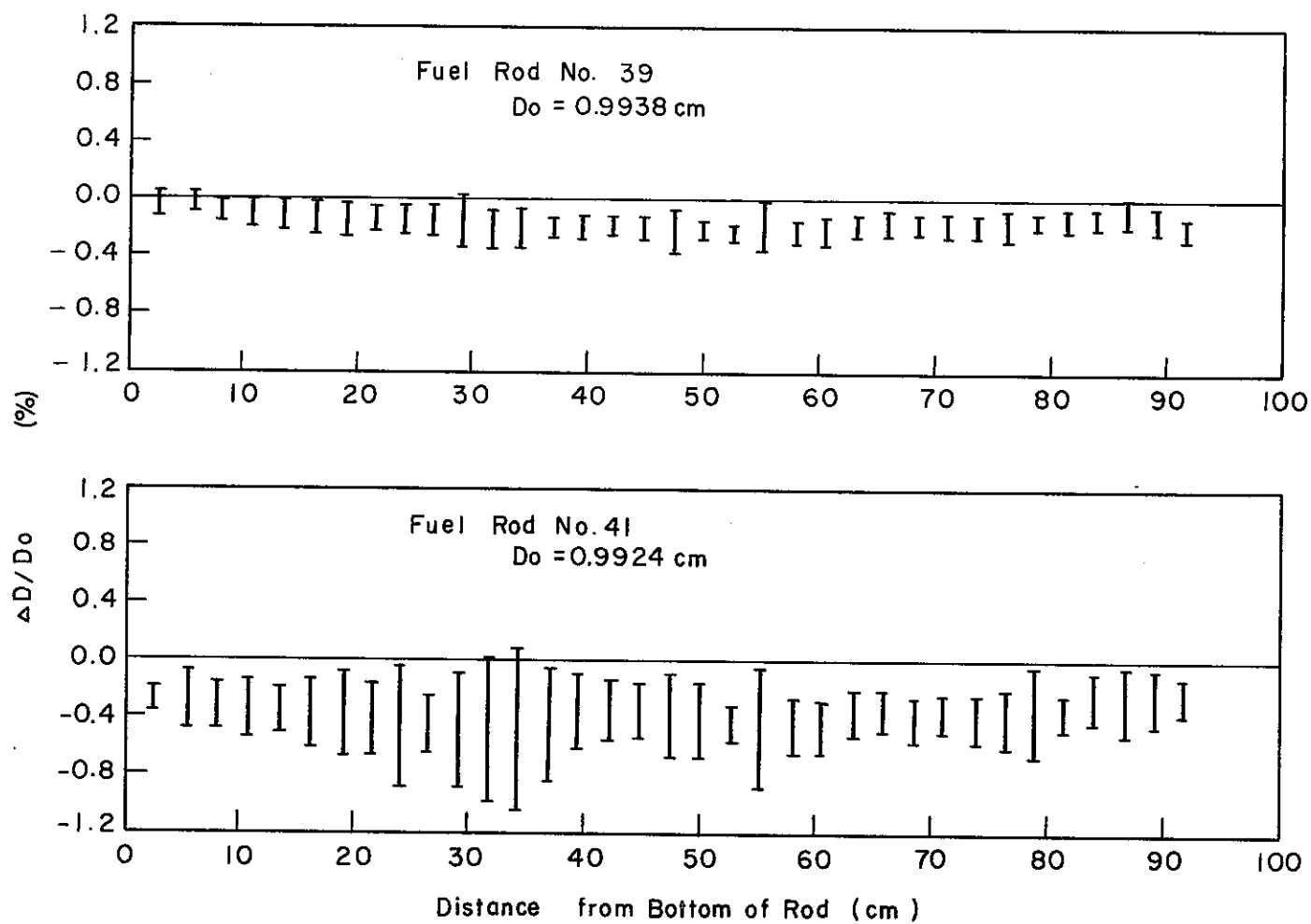


Figure 8. The Diameter Change of Rod No. 39 and 41

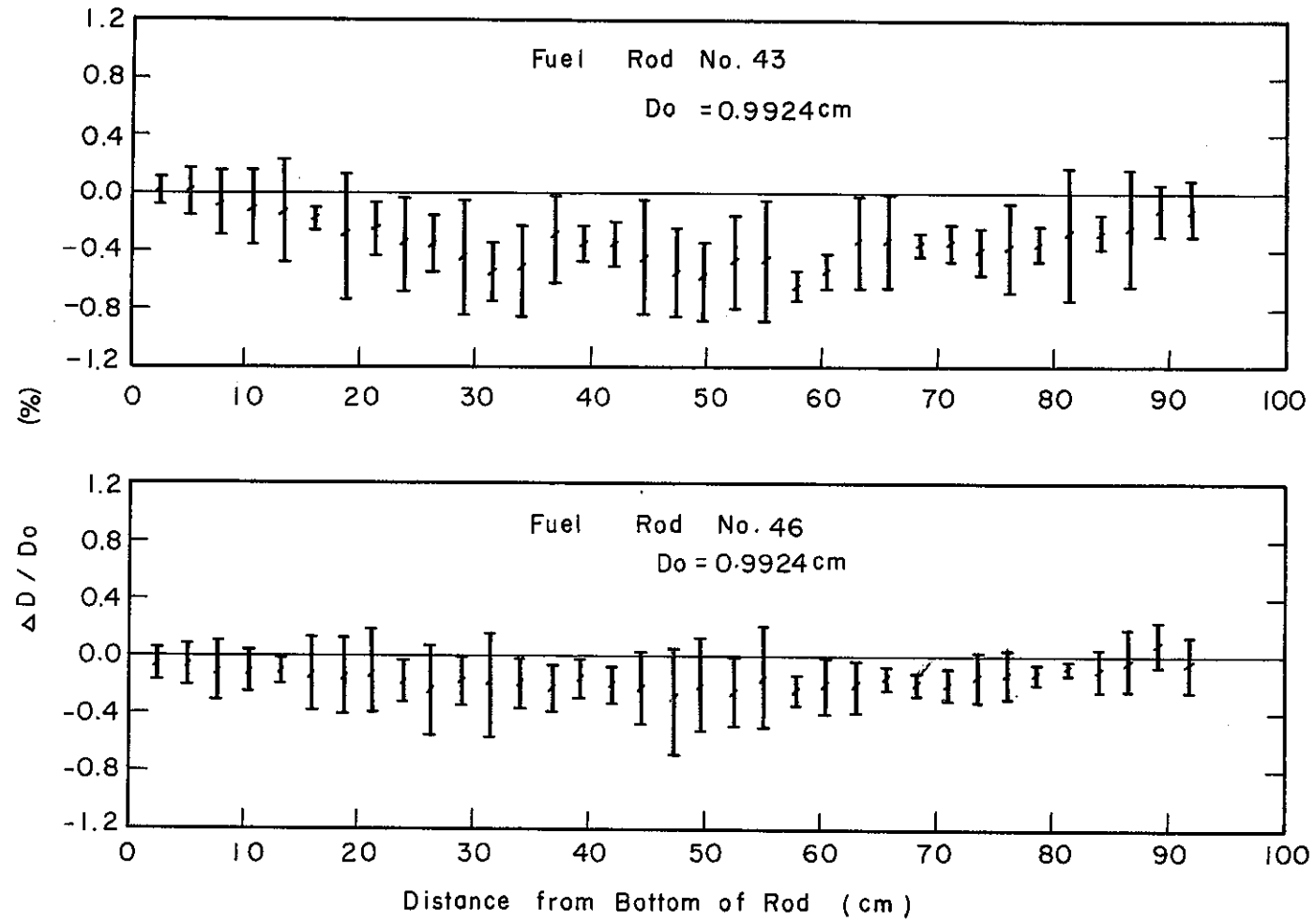


Figure 9. The Diameter Change of Rod No 43 and 46

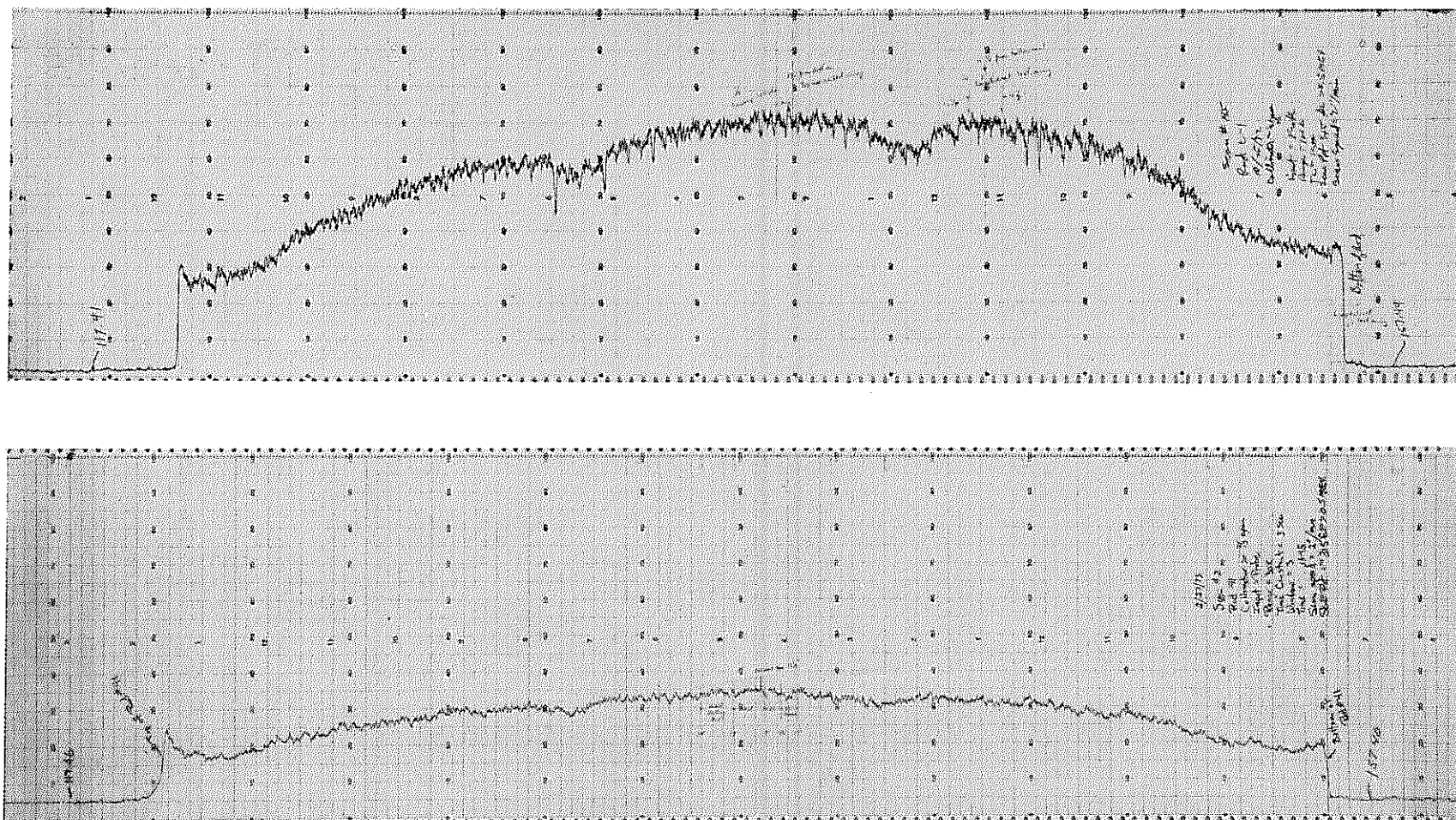
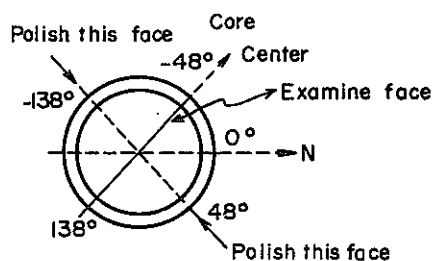
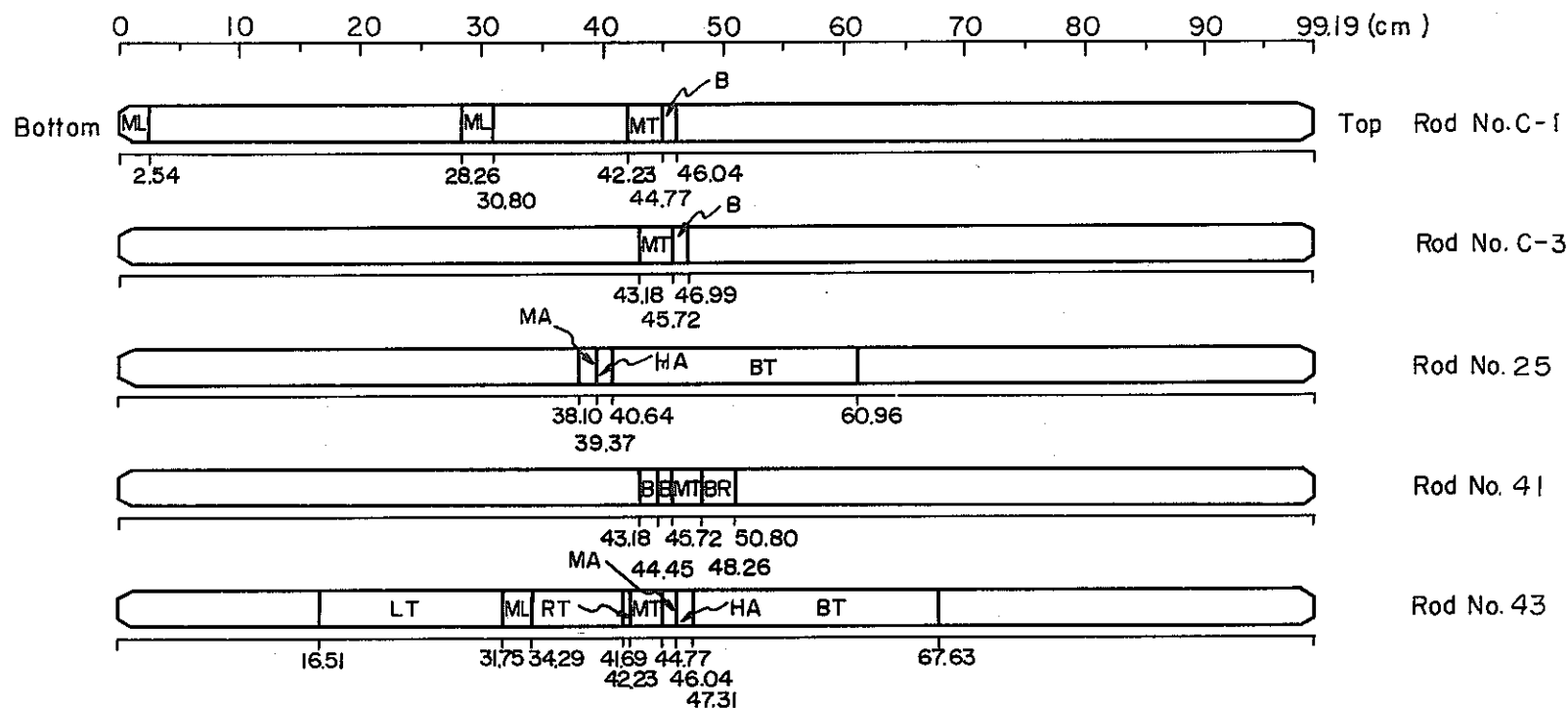


Figure 3. Gross Gamma Scanning Profiles of rods C-1 and 41



Note A: Examine face of longitudinal metallography

- ML ..... Clad & Fuel Metallography Sample Longitudinal Examine face Note A
- MT ..... Clad & Fuel Metallography Sample Transverse Examine face
- B ..... Burnup Sample
- MA ..... Clad Mn-54 Analysis Sample
- HA ..... Clad H<sub>2</sub> Analysis Sample
- BT ..... Clad Burst Test Sample
- BR ..... Burnup (Radial Drilling) Sample
- LT ..... Clad Longitudinal Tensile Test Sample
- RT ..... Clad Ring Tensile Test Sample

Figure 11. Post-Irradiation Examination Sectioning

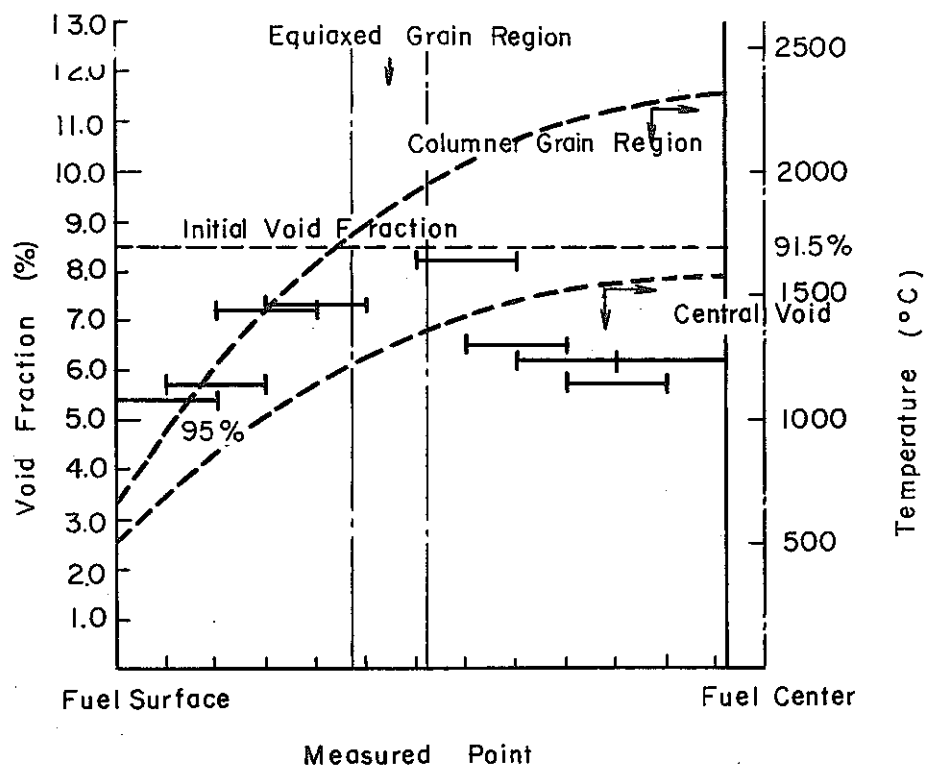


Figure 12 Temperature and Void Distribution of Rod No.C-1(Transverse Section)

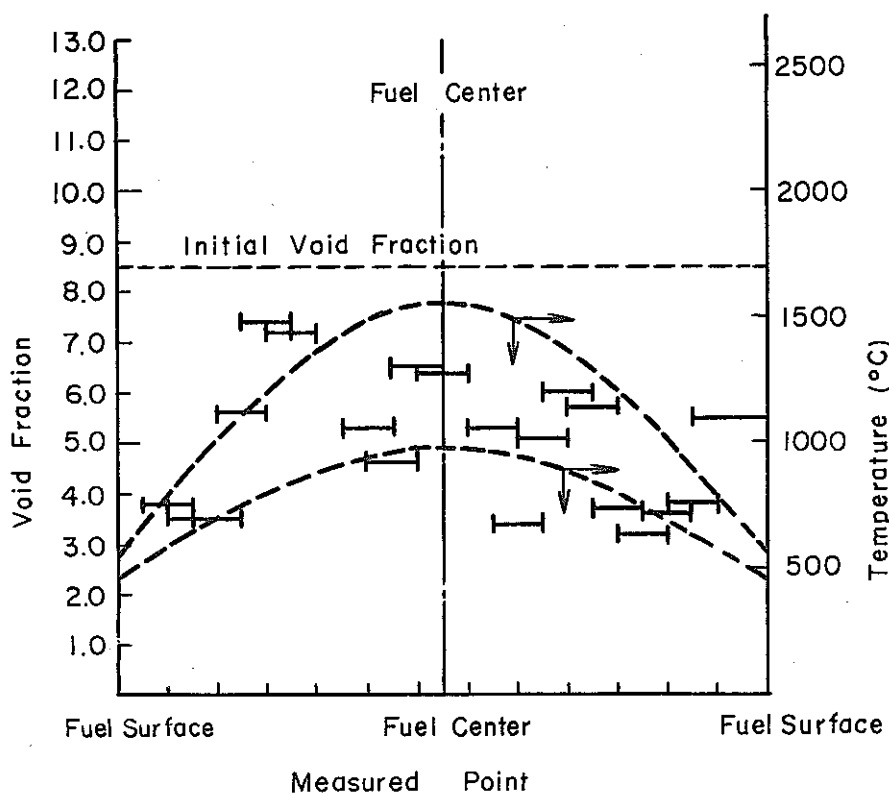


Figure 13 Temperature and Void Distribution of Rod No.C-3 (Transverse Section)

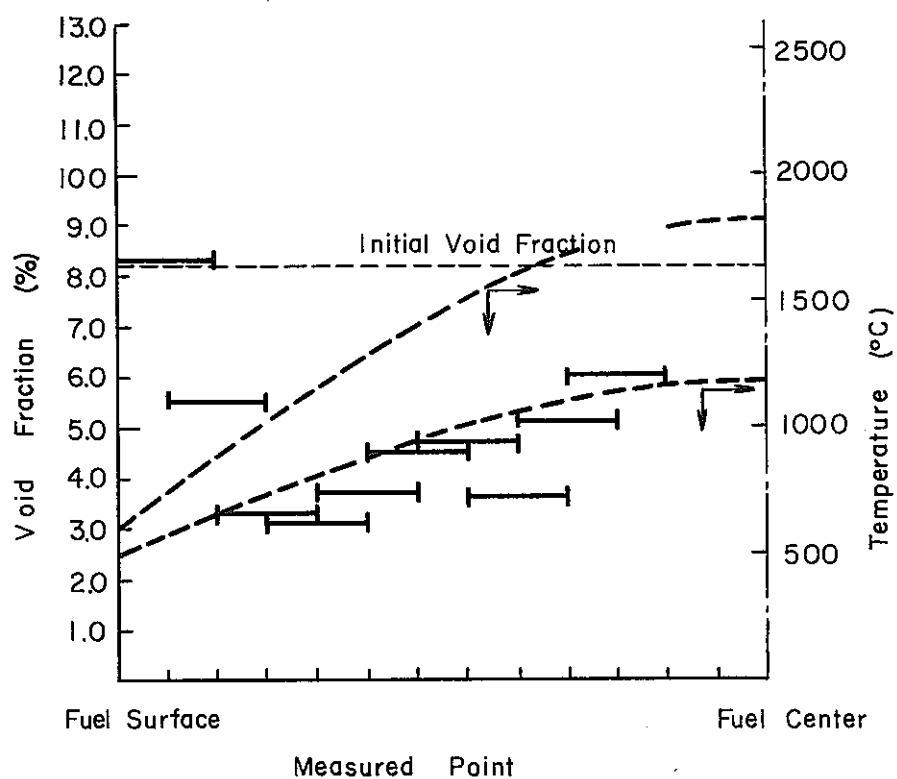


Figure 14. Temperature and Void Distribution of Rod No.43 (Transverse Section)

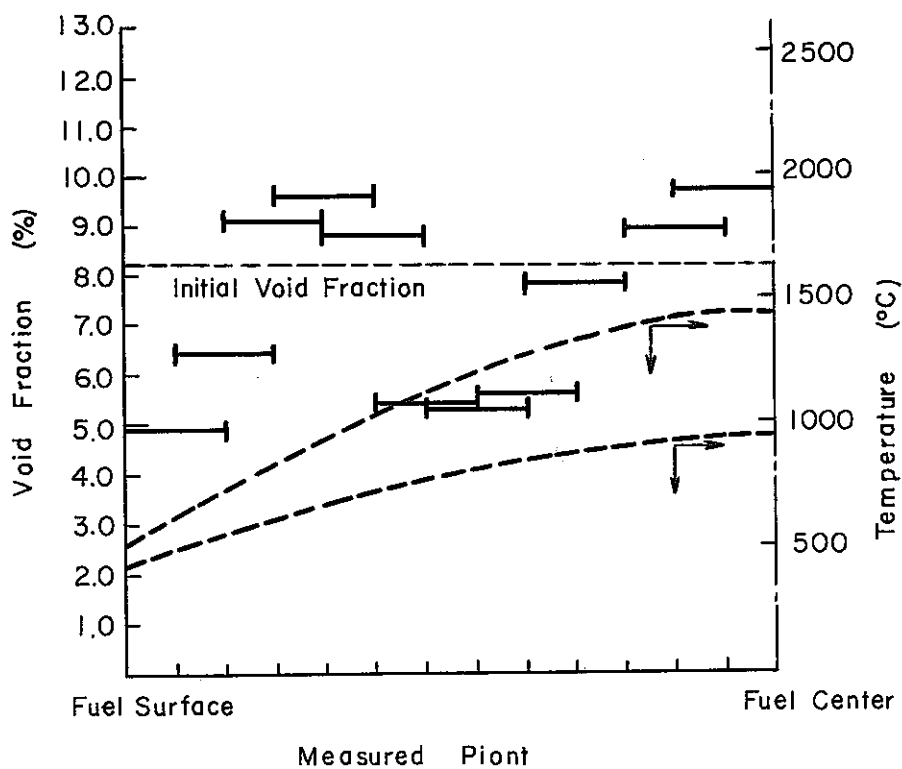


Figure 15. Temperature and Void Distribution of Rod No.43 (Longitudinal Section)

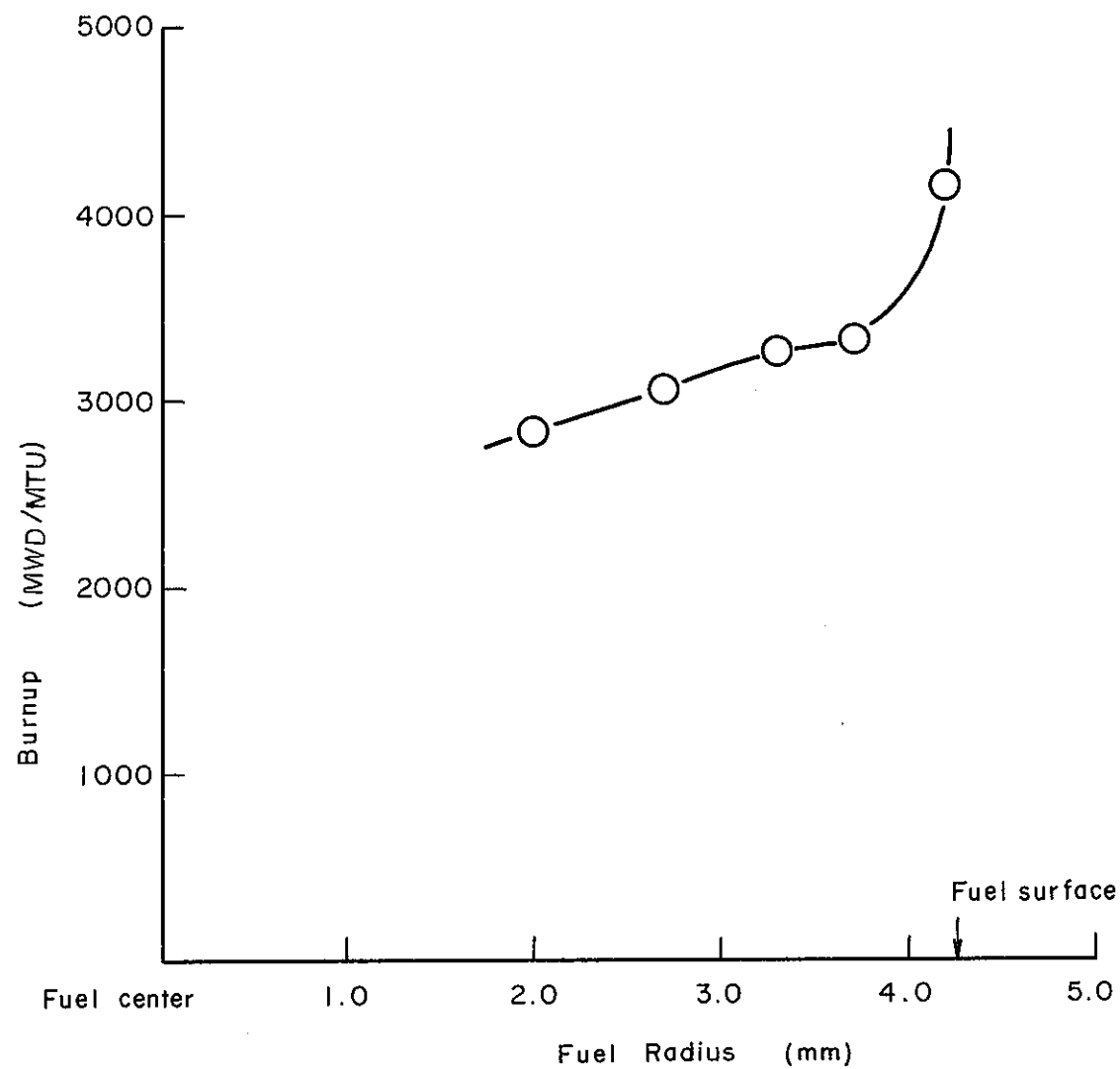


Figure. 16. Burnup Radial Distribution of Rod No.41



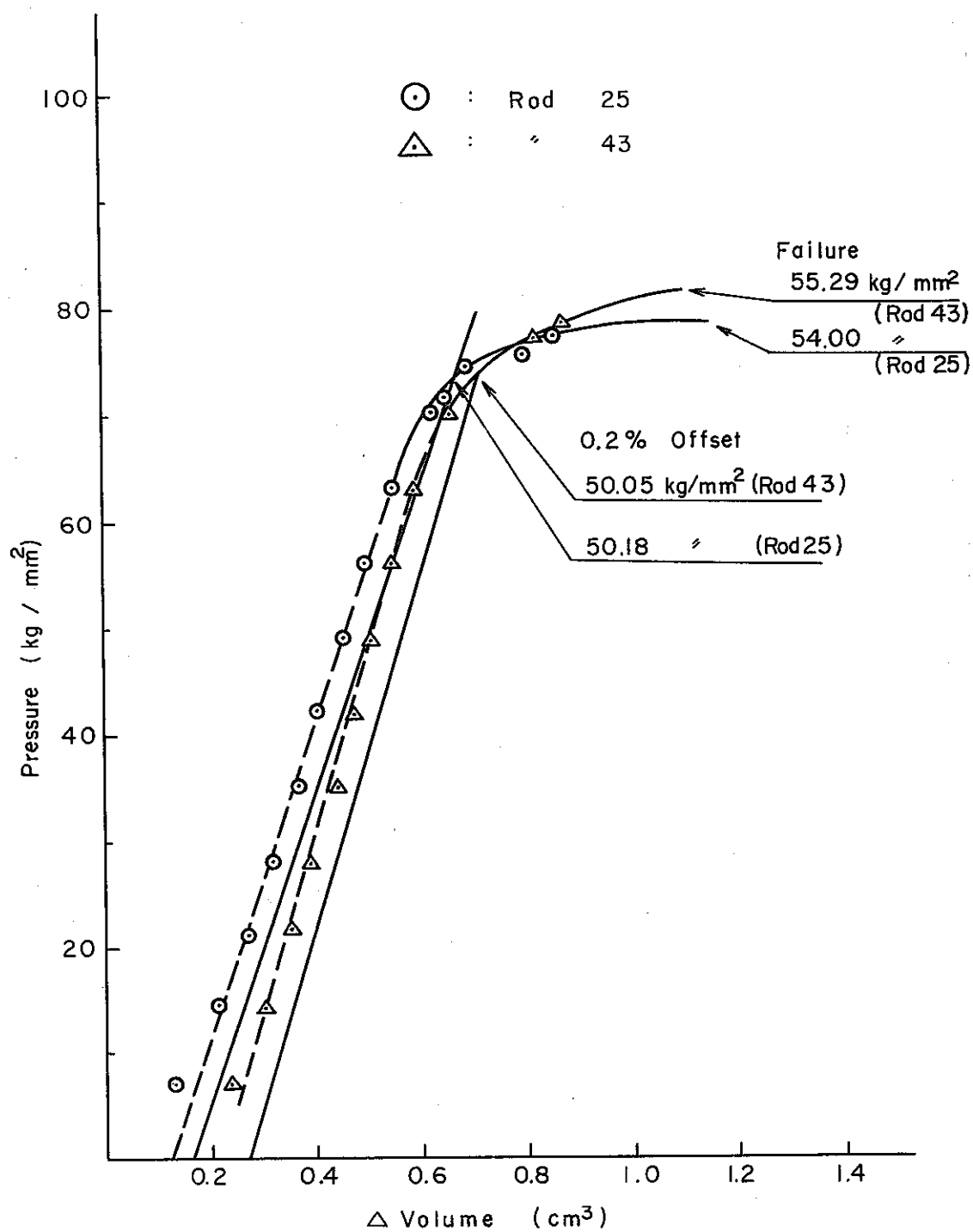


Figure 17. Pressure-ΔVolume Curve

Photo

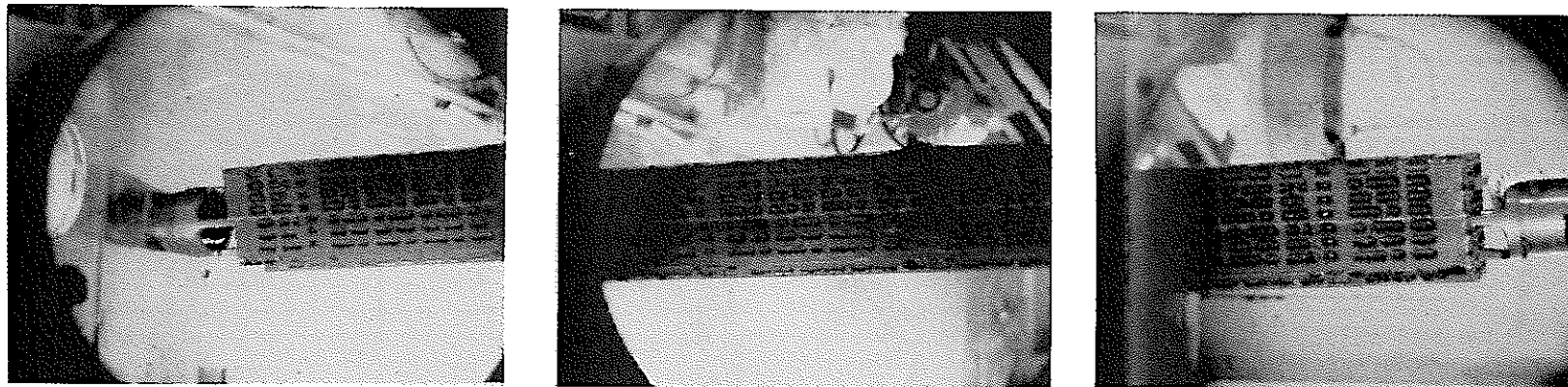
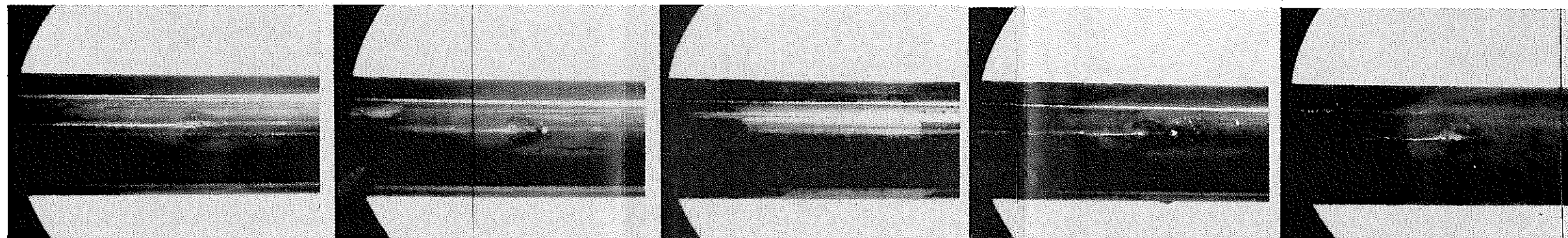
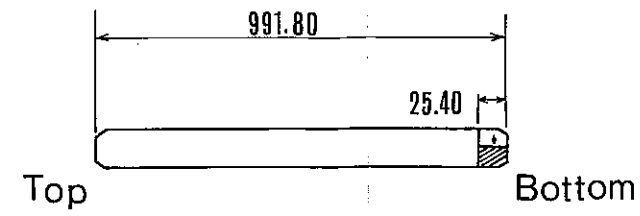
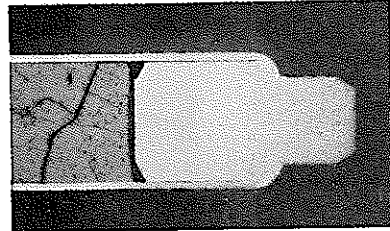


Photo-1 The View of PNC Assembly after Irradiation



11.43 cm From Bottom    36.83 cm From Bottom    49.53 cm From Bottom    62.23 cm From Bottom    87.63 cm From Bottom

Photo-2 The View of Rod No.41 after Irradiation



Top

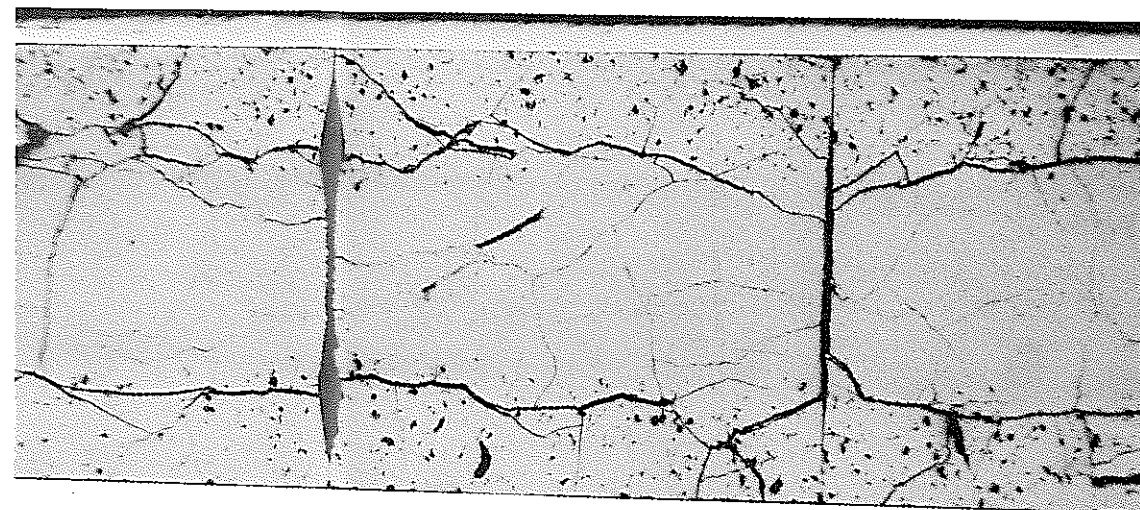
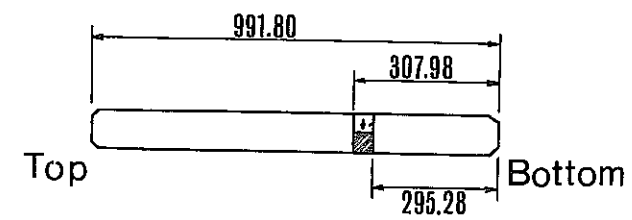
Bottom

Etched

x100

200  $\mu$

Photo - 3 Bottom End Cap - Clad Weld Area Macrography Rod No. C - 1



Top

Bottom

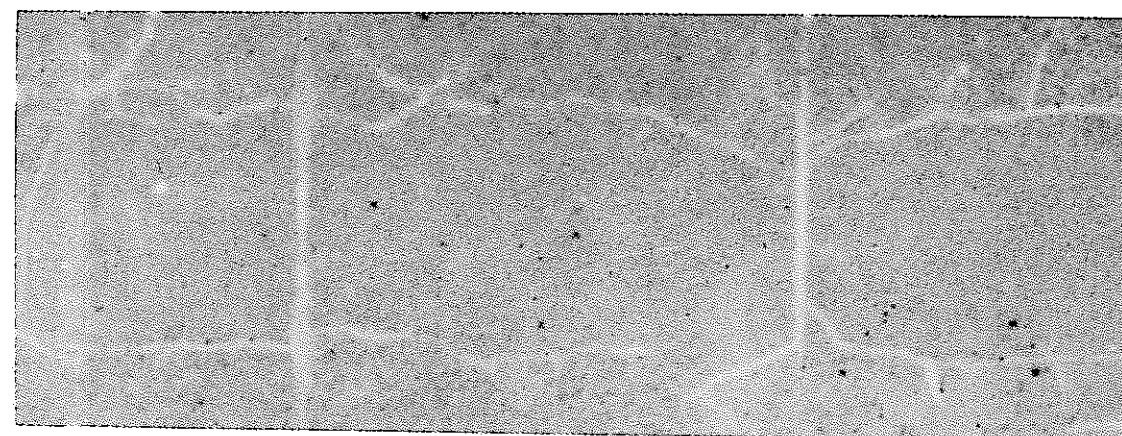
Macrography



Top

Bottom

$\beta-\gamma$  Autoradiography



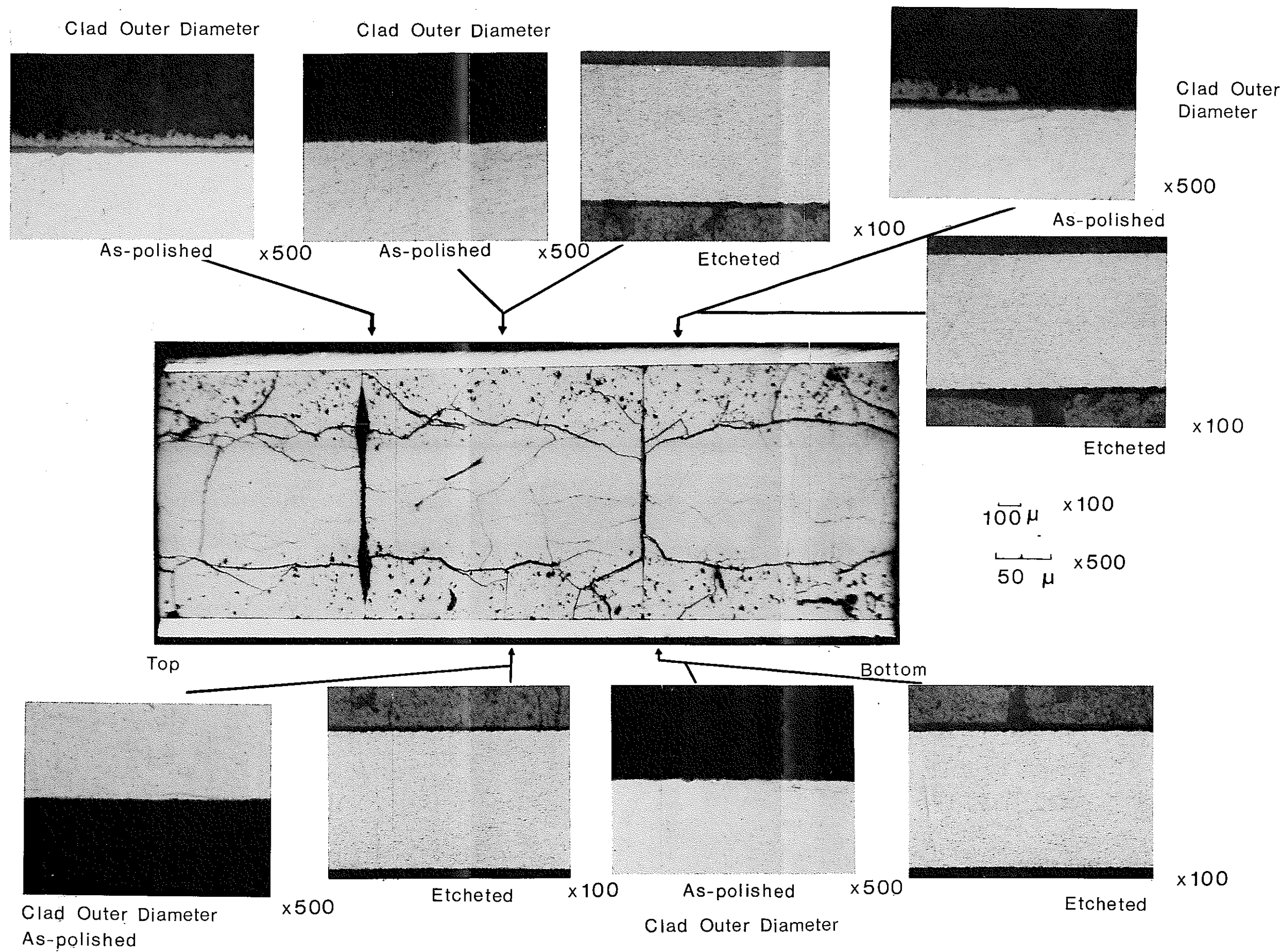
Top

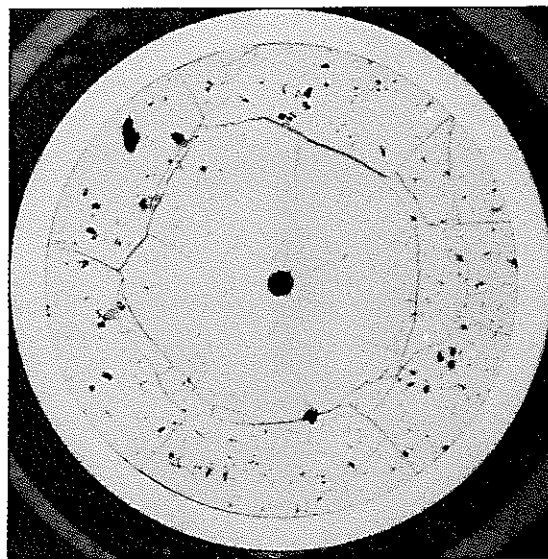
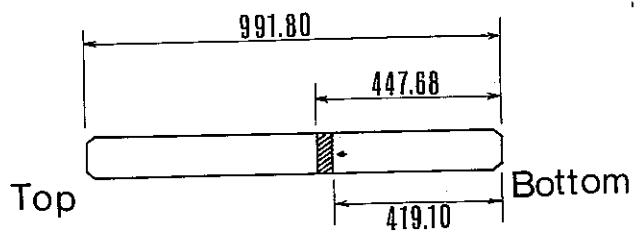
Bottom

$\alpha$  Autoradiography

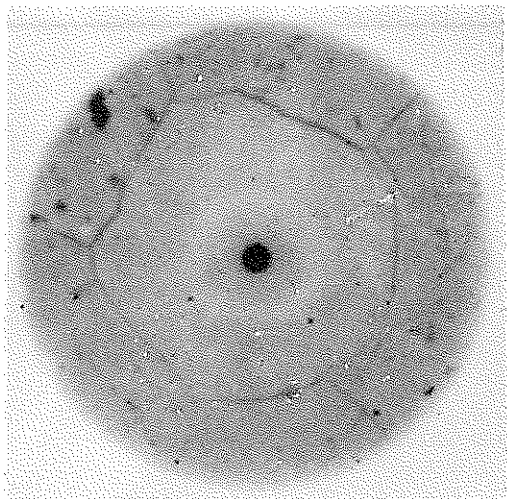
Photo-4 Macrography and  $\alpha, \beta-\gamma$  Autoradiography Rod No. C-1 (Longitudinal)



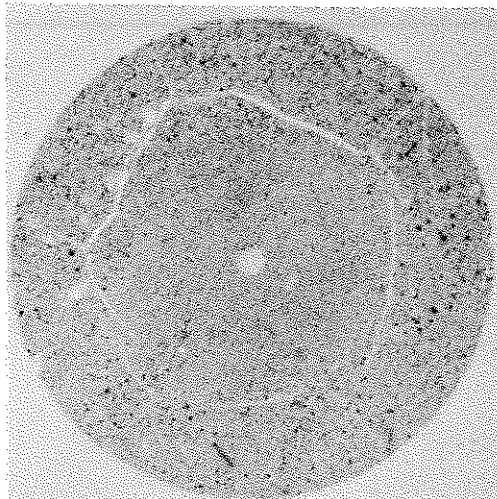




Macrography



Beta-Gamma



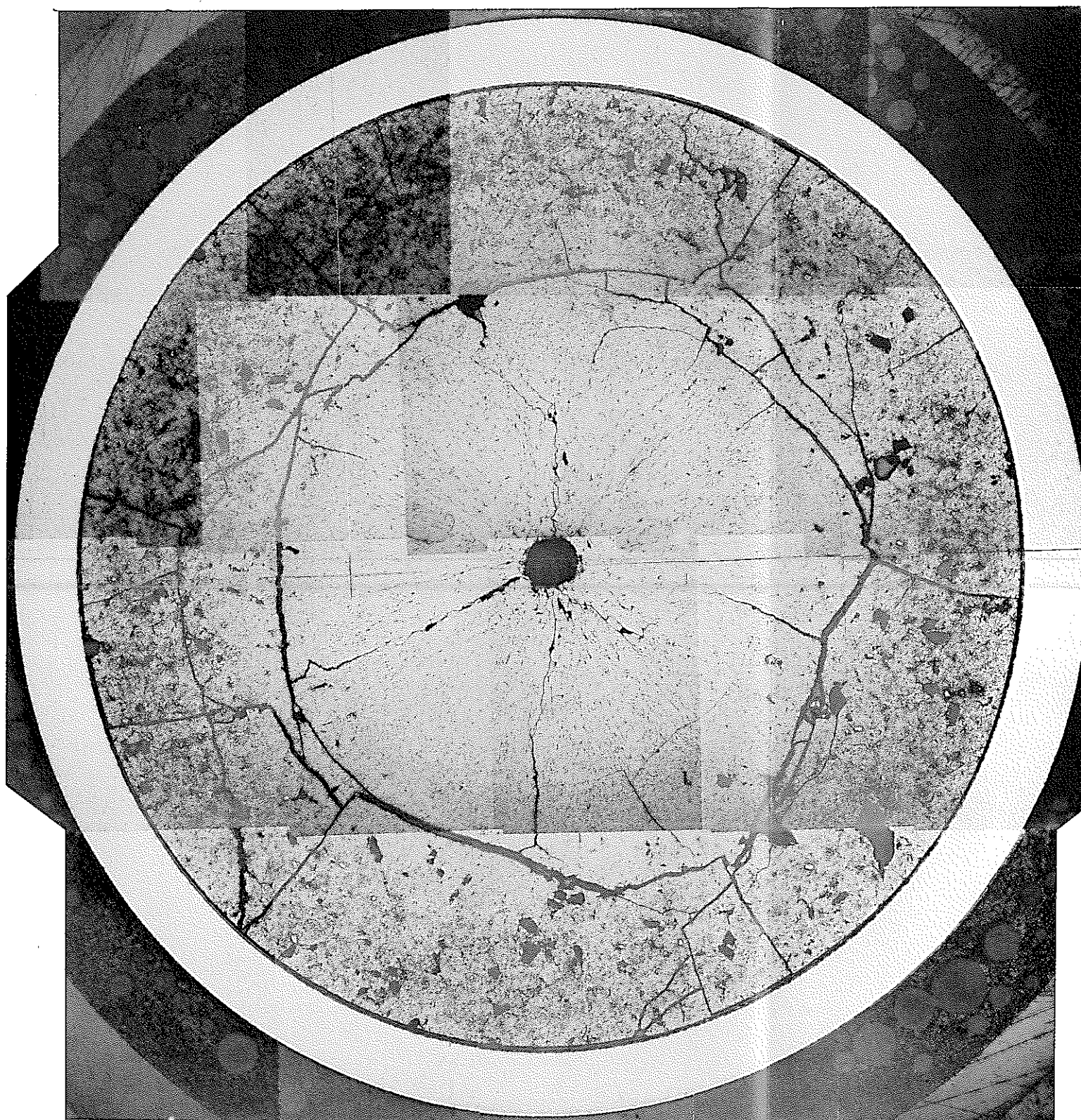
Alpha

Autoradiography

Photo - 1. Macrography and  $\alpha$ ,  $\beta$ - $\gamma$  Autoradiography

Rod No. C - 1





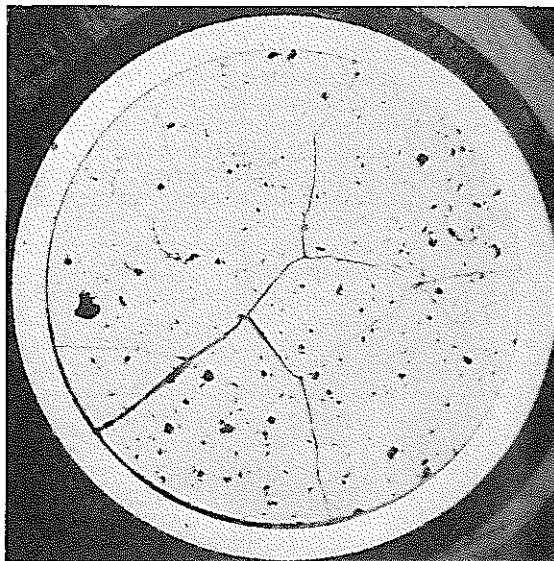
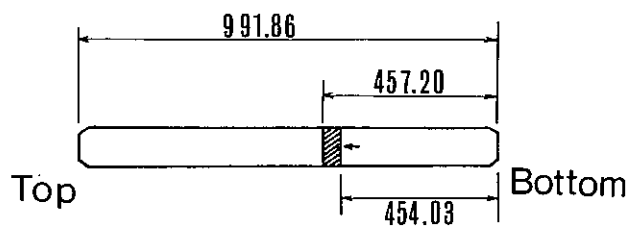
Etched

x 40

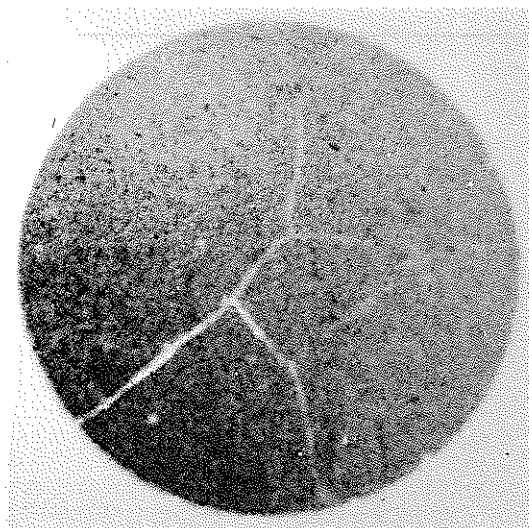
500  $\mu$

Photo - 2. Low Magnification Composite Rod No. C-1

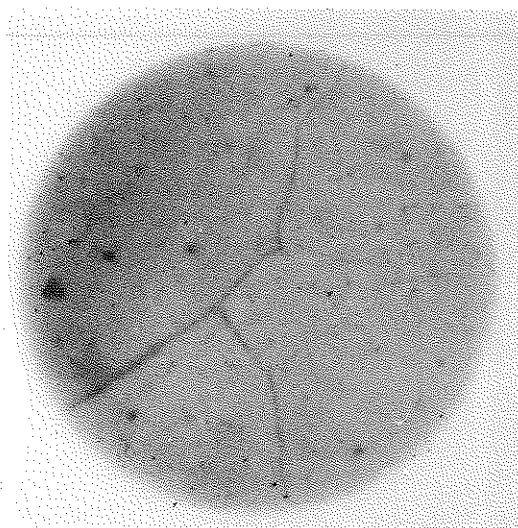




Macrography  
As-polished



Alpha

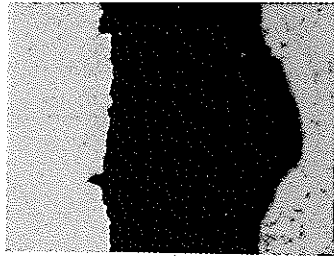


Beta- Gamma

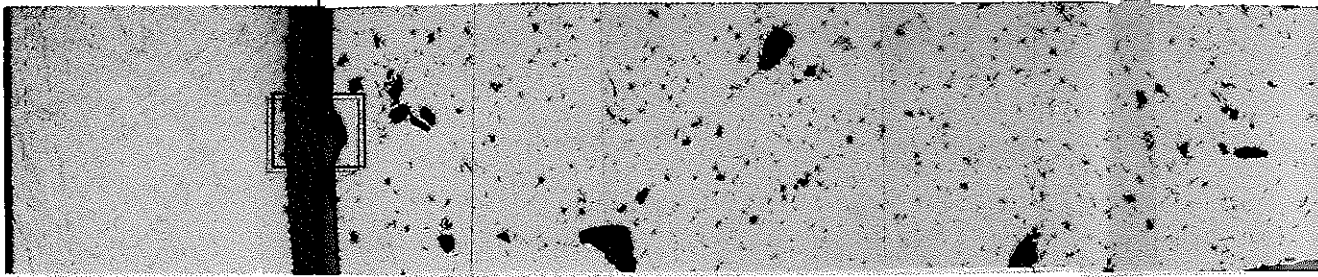
Autoradiography

Photo-8 Macrography and  $\alpha, \beta-\gamma$  Autoradiography

Rod No.C-3

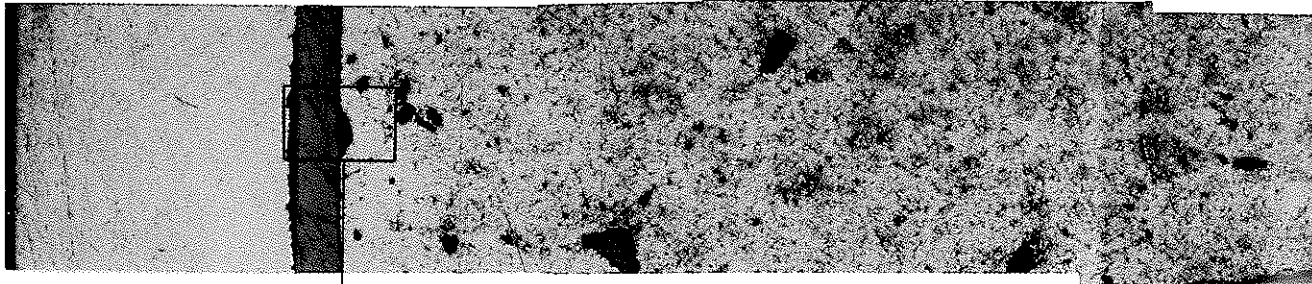


x500



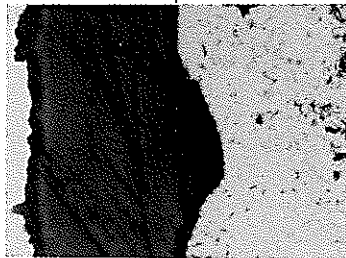
As-polished

x150



Etched

x150



x500

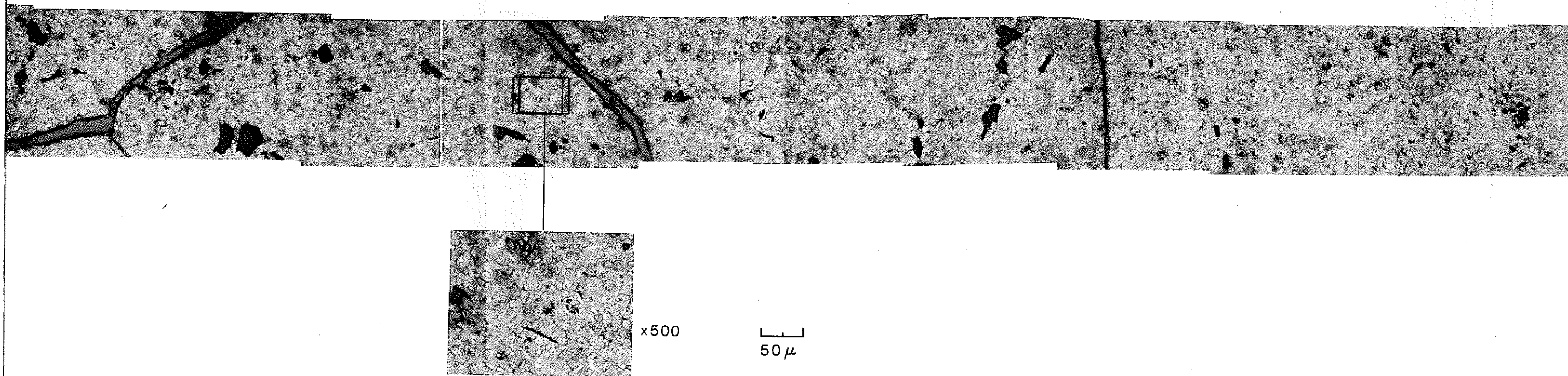
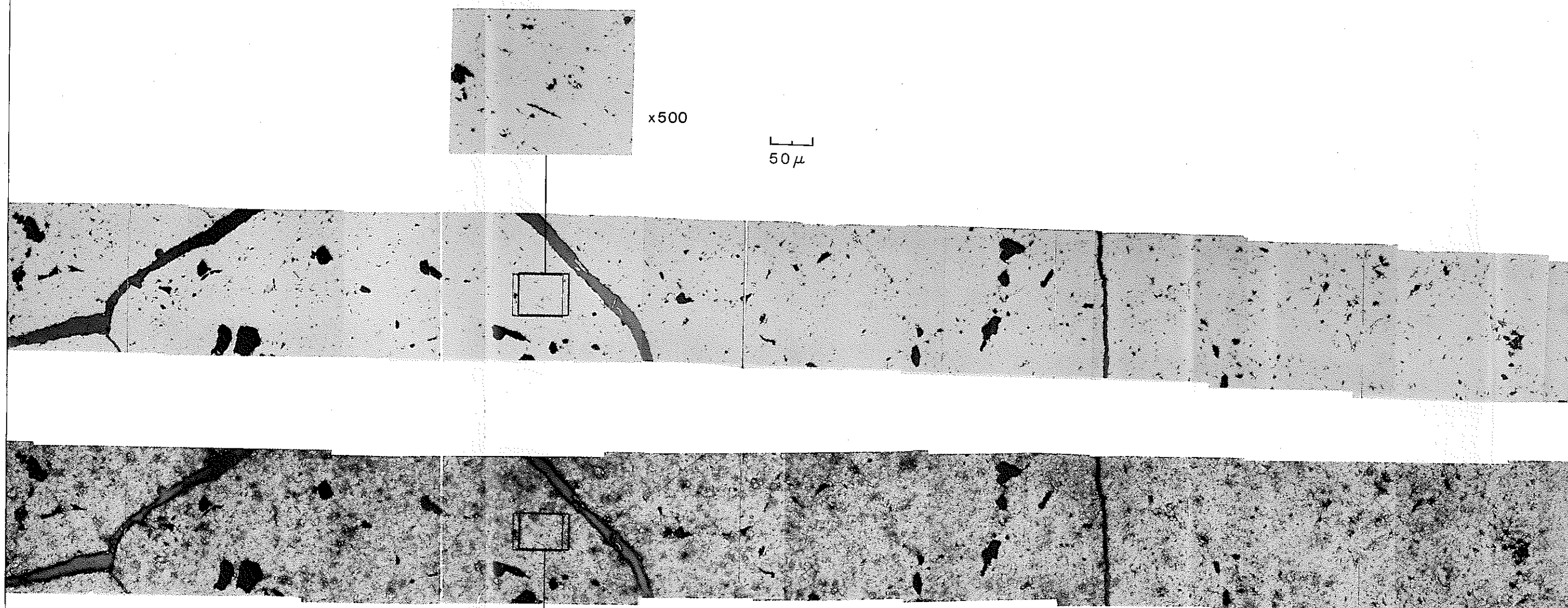
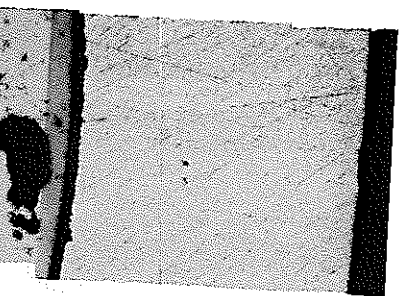
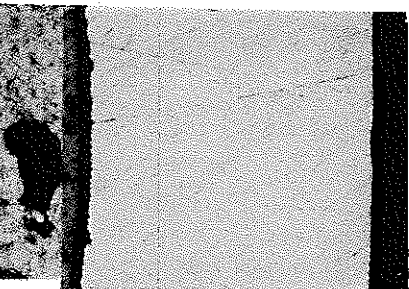
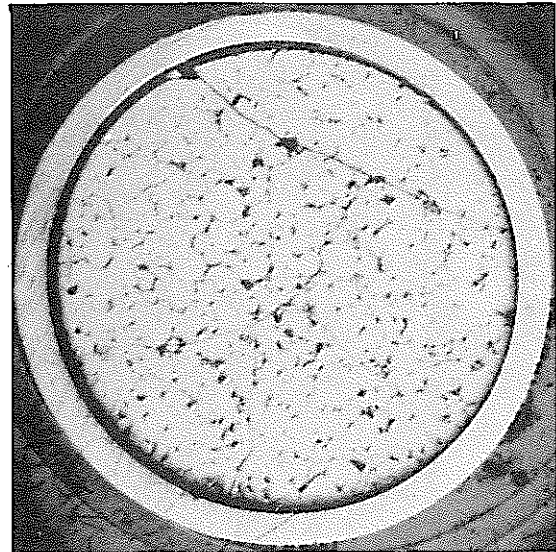
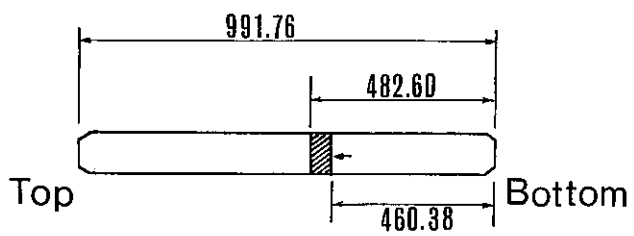


Photo-9 Transverse Section Rod No. C-3

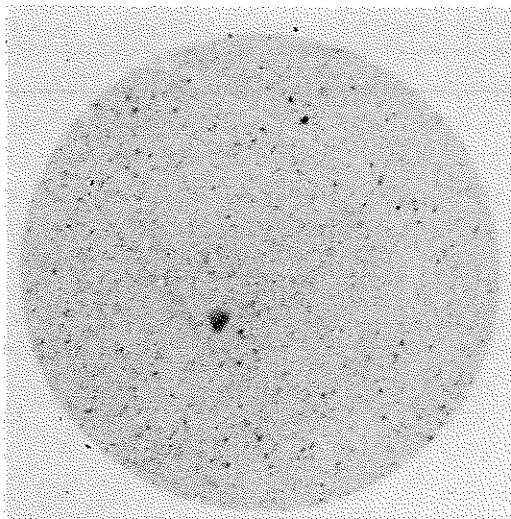


0.2 mm

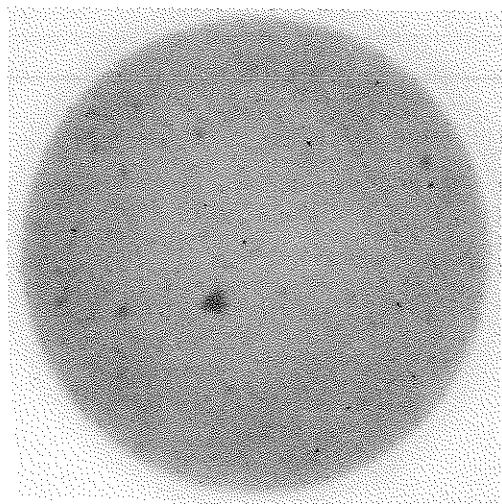




Macrography



Beta- Gamma



Alpha

Autoradiography

Photo-3. Macrography and  $\alpha, \beta - \gamma$  Autoradiography  
(Transverse) Rod No. 41



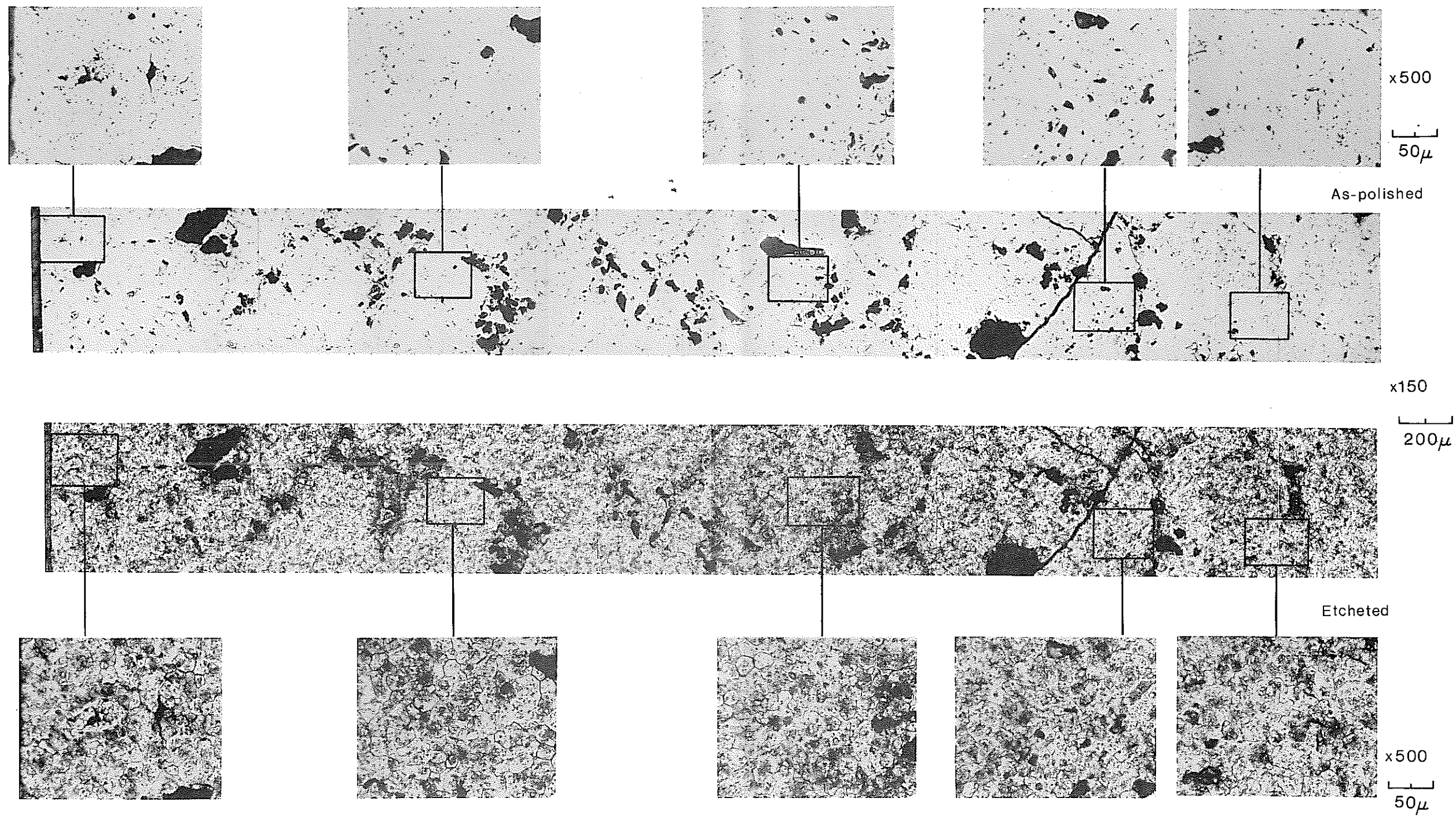
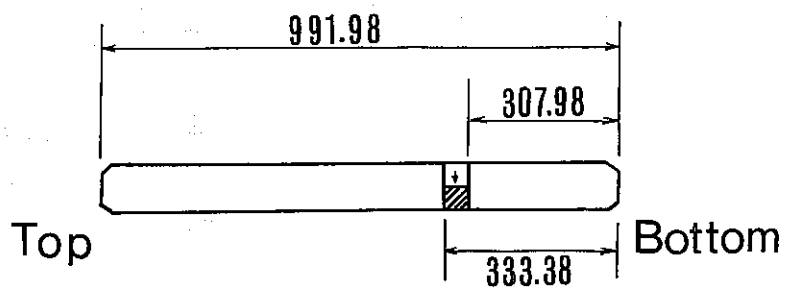
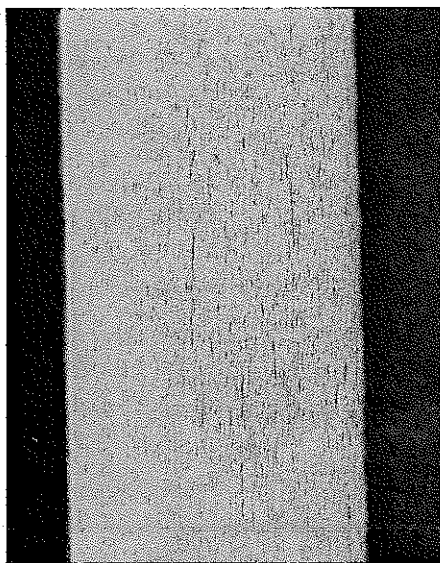


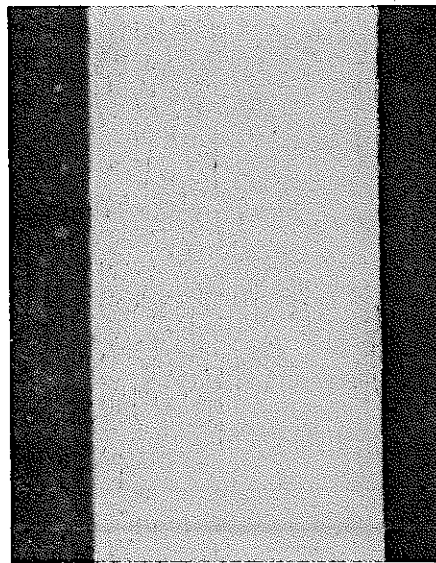
Photo-4. Transverse Section Rod No. 41



Top

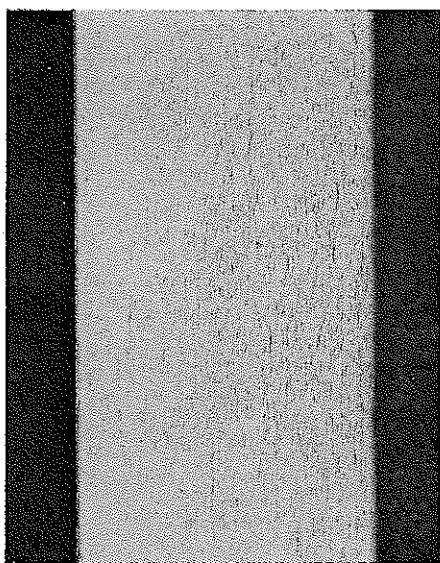


0°

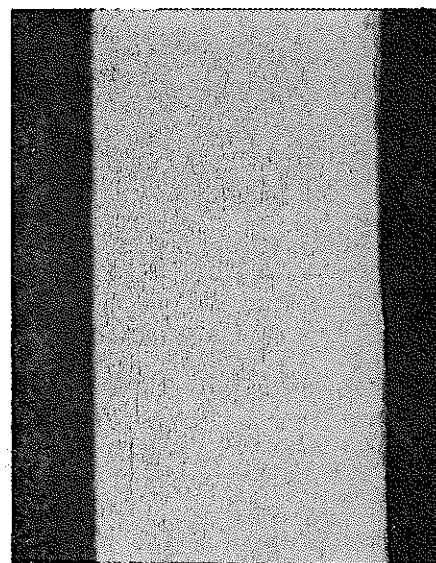


180°

Bottom



0°



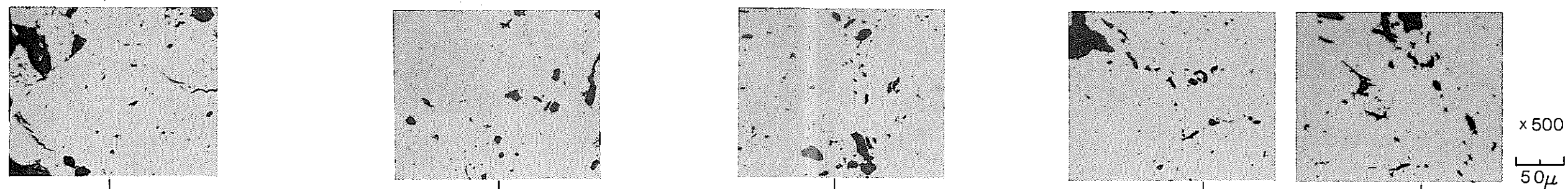
180°

Etched x100

200  $\mu$

Photo-12 Clad Micrography (Longitudinal) Rod No.43

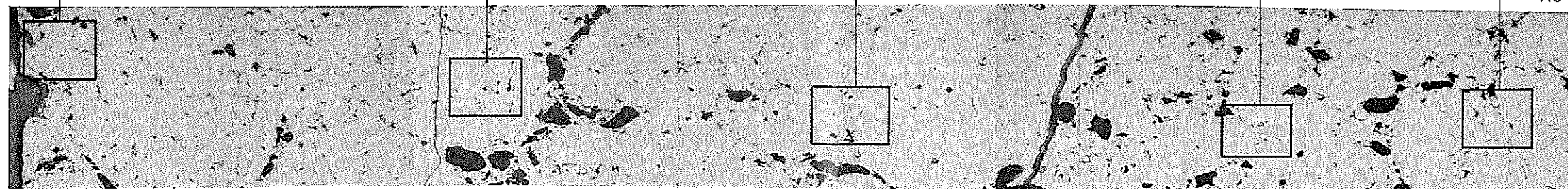




x 500

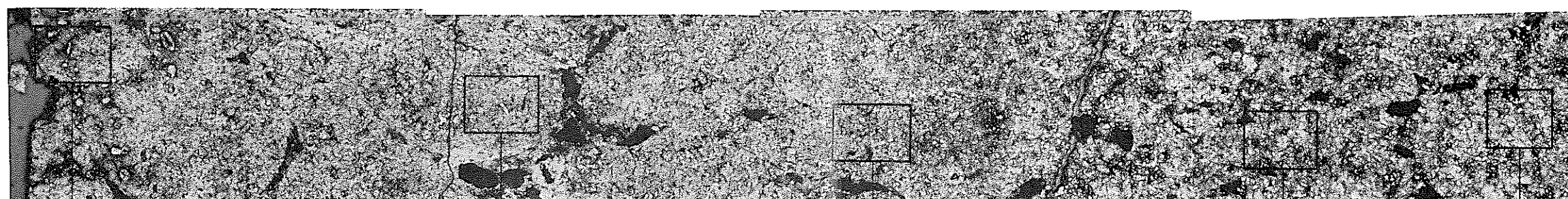
50μ

As-polished

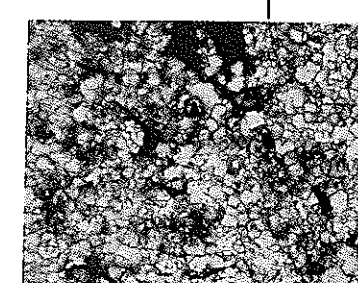
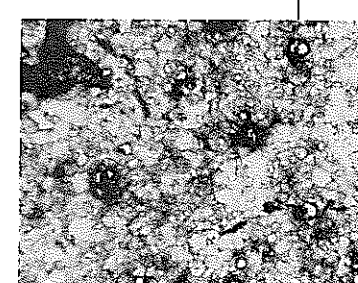
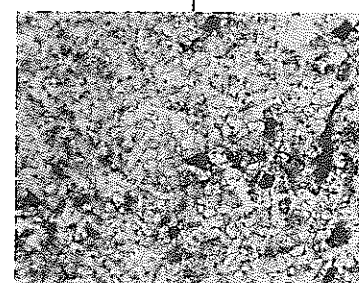
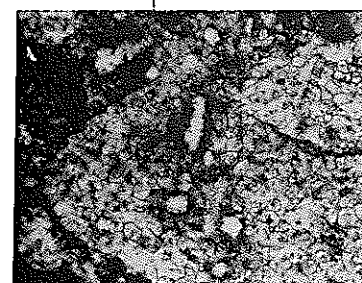


x150

200μ



Etched

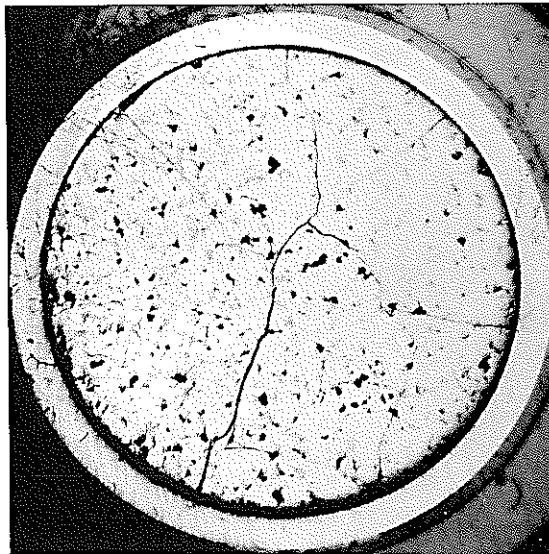
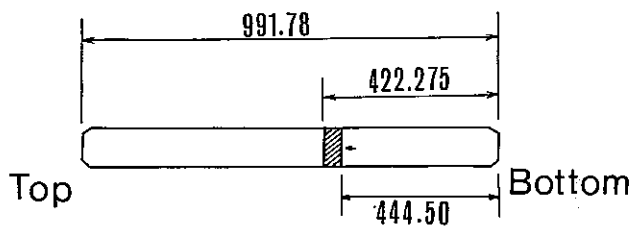


x 500

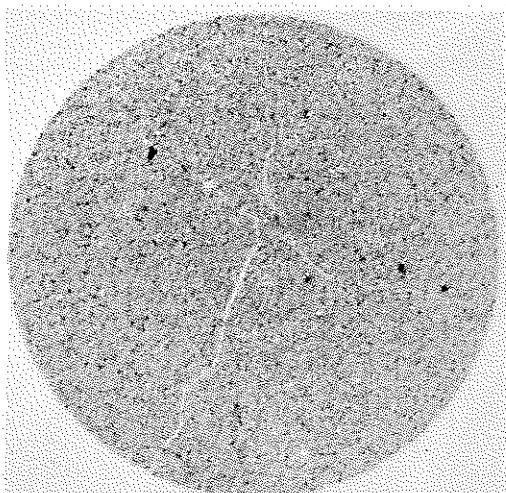
50μ

Photo-13 Longitudinal Section Rod No. 43

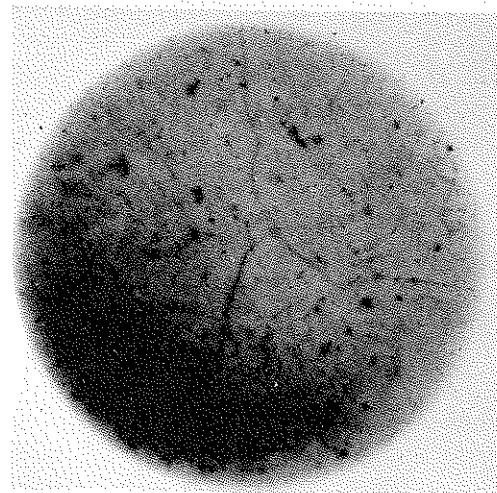




Macrography



Beta-Gamma



Alpha

Autoradiography

Photo-14 Macrography and  $\alpha, \beta-\gamma$  Autoradiography  
(Transverse) Rod No. 43

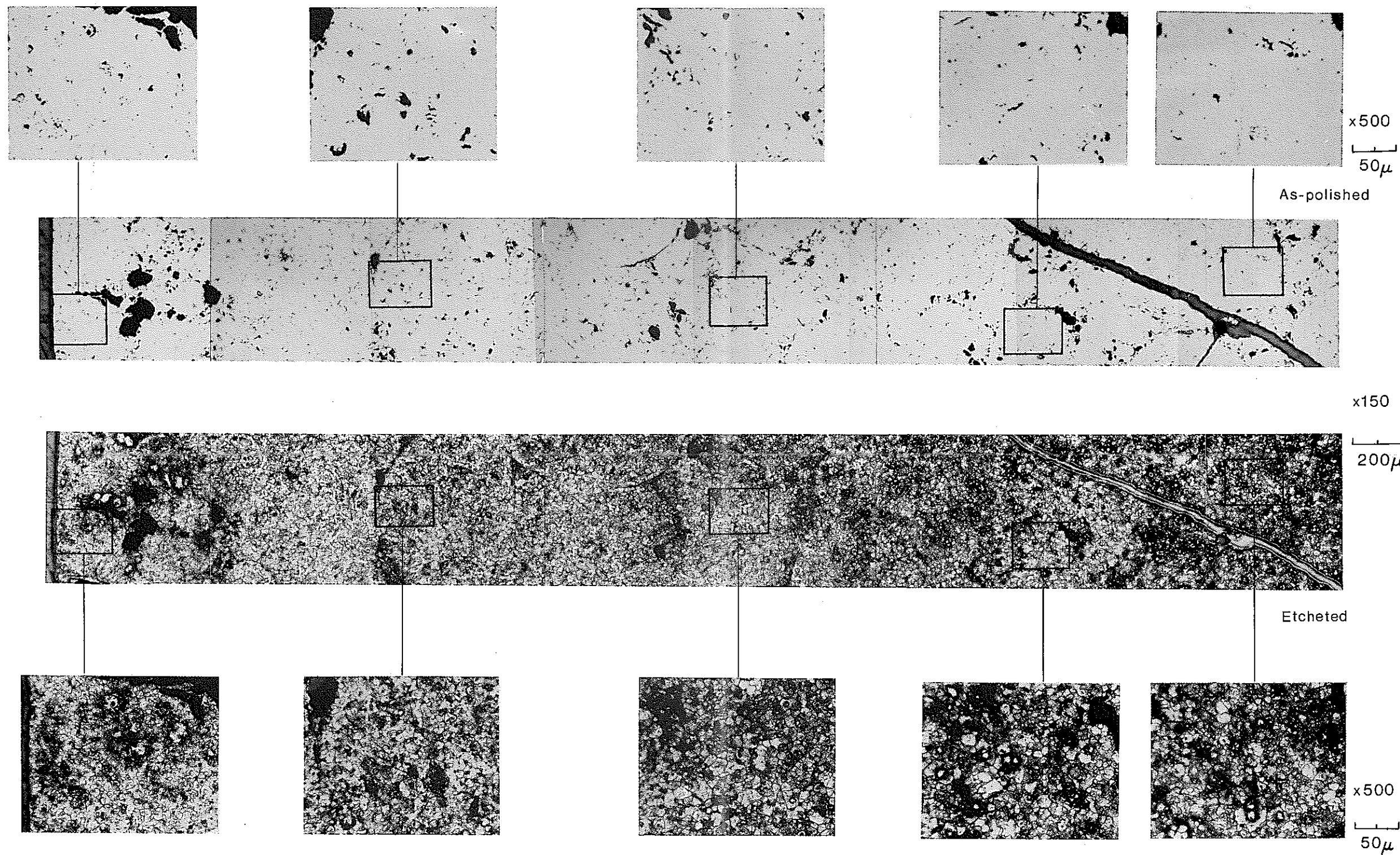


Photo-15 Transverse Section Rod No. 43